Entanglement dynamics of many-body quantum states with evolving system conditions

Devanshu Shekhar and Pragya Shukla

Department of Physics, Indian Institute of Technology,

Kharagpur-721302, West Bengal, India

(Dated: March 5, 2025)

Abstract

The entanglement analysis of a pure state of a many-body quantum system requires a prior information about its density matrix/ state matrix, obtained in principle by solving the Hamiltonian matrix. The missing information due to complexity of the many-body interactions however renders it necessary to consider an ensemble of Hamiltonians and thereby an ensemble of pure states. This in turn leaves a statistical description of the entanglement measures as the only option.

We consider physical Hamiltonians that can be modelled by a multiparametric Gaussian ensembles, theoretically derive the state ensembles for its eigenstates and analyze the effect of varying system conditions on its entanglement statistics. Our approach leads to a single parametric based common mathematical formulation for the evolution of the statistics of different state ensembles. The parameter turns out to be a single functional of the system parameters and thereby reveals a deep web of connection underlying different quantum states.

I.   INTRODUCTION

An important requirement of quantum information processing is that any knowledge of the many-body state provides minimum information about its subunits. One way to ensure this is by maximizing the amount of entanglement among the subunits; this in turn leads to a massive search for the states with maximum entanglement, e.g., an ergodic state (i.e. one accessing all parts of Hilbert space with equal probability). An arbitrary many-body state is however usually non-ergodic, with partial entanglement (lying between separability and maximum entanglement). The question is (i) how to quantify its entanglement? (ii) what type of variation of system conditions can lead to an enhancement of entanglement? (ii) whether its entanglement can be preserved in time or under changing system conditions once it reaches the maximum entanglement limit?

Notwithstanding intense research efforts in past two decades, a detailed theoretical formulation about the non-equilibrium dynamics of a quantum many-body system is still not available. The growth of entanglement among subunits with time also renders the analysis beyond the access of numerical techniques, e.g., the time-dependent density matrix renormalization group theory. This motivates us to seek new theoretical routes to investigate many-body entanglement and thereby gain insights in the non-equilibrium quantum dynamics.

In general, the interactions among various subunits of a many-body system are sensitive to a host of system conditions, both static as well dynamic type. A variation of these conditions can lead to changes in the mutual interactions among subunits. This in turn is expected to manifest in the behavior of a typical many-body state and thereby entanglement measures, more clearly if the dynamics is analyzed in a Hilbert space consisting of the eigenstates of the non-interacting Hamiltonian, i.e, product states of subunits. In general, it is desirable to determine the multi-partite entanglement (i.e. between its many parts) for a given set of system conditions as well its variation with changing interactions among various parts. The technical complexity further enhanced by a lack of unanimous accepted definition of entanglements measures renders the determination a very difficult task. Fortunately many important insights can still be achieved by consideration of the entanglement between its two sub-parts, referred as the bipartite entanglement,

The standard route to determine the entanglement measures for a pure state requires a prior knowledge of the density matrix $\rho = |\Psi\rangle\langle\Psi|$. The latter can in turn be obtained either by consideration of the state tensor determined through some information theoretic approaches, or by solving the eigenvalue equation for the Hamiltonian, determining its states and then calculation of the state matrix. Previous entanglement studies of pure random states in bipartite basis are either based on direct modelling of the state matrix ensemble, e.g., by a Ginibre ensemble leading to a stationary Wishart ensemble (e.g. [1–6]) or its generalizations, e.g., [7–9]. Although these studies provided many insights, they lacked a very important aspect: as the state matrix ensemble was derived without any reference to underlying Hamiltonian, the connection of ensemble parameters with system parameters was not explicit. This handicaps one from a direct analysis of the entanglement dynamics with changing system parameters. The primary objective of our present study is to fulfil this information gap.

To achieve our objective, we first need to determine the matrix representation of the Hamiltonian in a physically motivated basis and thereafter its eigenstates. A many-body Hamiltonian however consists of complicated interactions among its subunits which even if well-known, e.g., coulomb interactions, an exact determination of its matrix elements is not often possible; this could occur, for example, due to the technical issues involved in calculation of the integrals either by theoretical or numerical route. The incomplete knowledge or error in their determination manifests itself by randomization of the matrix elements. For

example, if the matrix element can be determined up to its average value and variance, the maximum entropy hypothesis predicts its distribution to be a Gaussian. An availability of information about higher order moments can lead to non-Gaussian distributions and conservation laws can result in correlated distributions. Besides not all elements need be random, some of them can be exactly determined. For example, for Hamiltonian of a tight binding lattice with onsite disorder and nearest neighbor hopping, the diagonals in a site basis are randomly distributed and the off-diagonals are all non-random (given by hopping strength). Indeed, the nature and type of the distribution of the matrix elements is sensitive to various system conditions, e.g., symmetry and conservation laws, dimensionality and boundary conditions, disorder etc. and can vary from one element to the other. As a consequence, the Hamiltonian matrix is best represented be a system-dependent random matrix, with some or all elements randomly distributed. The information about the system appear through the distribution parameters.

As expected, the randomness underlying the matrix elements also manifests in the eigenstates of the Hamiltonian and the distribution of the latter can be derived, in principle, from the JPDF of the former by a transformation of variables from matrix space to eigenvalue-eigenstate space. The information in turn leads to the statistical behavior of the entanglement measures. An integration of the ensemble density of the Hamiltonian , i.e, the JPDF of the matrix elements is in general technically complicated, thus motivating a search for alternative routes, e.g., a differential route. As discussed in [10], an evolution equation for the JPDF of the components of an arbitrary eigenstate (referred as state JPDF hereafter for brevity) for a many-body system represented by multiparametric Gaussian ensembles can be derived from the ensemble density. An additional benefit of the differential route is a common mathematical formulation, later referred as the complexity parameter formulation, of the state JPDF for a wide range of many-body systems where the system information is contained in a single parameter, i.e., the complexity parameter. We apply the complexity parameter formulation in the present work and derive the evolution equation for the entanglement measures and their solutions.

We proceed as follows. The statistical analysis of the static as well as dynamic properties of a M rank random tensor is although very desirable but technically complicated. Fortunately it is possible to gain many insights in the entanglement aspects of an eigenstate of a many-body Hamiltonian, say H, by dividing the whole system in two parts or by considering

a 2-body Interaction. As our primary focus here is to derive the evolution equation for the entanglement entropy of the eigenstate, it depends on following steps: (i) derivation of the diffusion equation for the matrix elements of H, (ii) derivation of the evolution equation for the eigenfunction components, (iii) determination of the moments of the JPDF of the reduced density matrix elements and thereby of Schmidt eigenvalues, (iv) derivation of the evolution equation for the entanglement entropy and purity of a wide range of the non-ergodic states. Using separable state as the initial condition, the equation can be solved to give the ensemble averages of the entanglement entropy and purity.

The paper is organized as follows. We begin, in section II, with two examples of prototypical Hamiltonians, namely (i) a many body Hamiltonian modelled by a generalized version of random energy model and (ii) a single particle Anderson Hamiltonian, and, their ensemble densities and the relation between system parameters and ensemble parameters. The latter is needed to analyze the effect of changing system conditions on the ensemble parameters. Section III describes briefly necessary tools for our approach, i.e, the diffusion equation for the ensemble density of a many body Hamiltonian in terms of changing ensemble parameters. This is necessary to derive the matrix elements moments used, in section IV, to derive the diffusion equation for the components of an arbitrary many-body state. (As discussed in [10], the equation can also be derived by a direct integration of the Hamiltonian ensemble density). Section V presents a calculation of the average entanglement measures namely von-Neumann entropy and purity for bipartite states with varying system conditions; we find that the result in infinite size limit is almost same as those obtained by a direct modelling of the state matrix ensemble. Section VI derives a formulation for the single particle entanglement entropy, a relevant tool to analyze the entanglement between two modes wherein the particle occupies either the part A or B of the lattice. Based on the two systems mentioned in section II, we pursue a numerical verification of our theoretical predictions and find a good agreement; this is described in section VII. We conclude in section VIII with a summary of our ideas, results and open questions.

II.   HAMILTONIAN AND ENSEMBLE DENSITY

Consider a many-body system in a pure state $|\Psi\rangle$. The information about the quantum correlations between the two sub-parts is contained in the components of $|\Psi\rangle$ represented

in the bipartite basis, consisting of orthonormal bases of the two sub parts. Assuming the orthogonal subspaces of its sub parts A and B, consisting of basis vectors $|a_k\rangle$ and $|b_l\rangle$, $k = 1 \rightarrow N_A, l = 1 \rightarrow N_B$ respectively, we can write $|\Psi\rangle = \sum C_{kl} |a_k\rangle |b_l\rangle$; the matrix with coefficients C_{kl} (complex or real) as its entries is referred as the state matrix. The standard entanglement measures for a pure bipartite state, viz., the von Neumann R_1 and other Rényi entropies R_n with $n > 1$, are functions of the eigenvalues of the $N_A \times N_A$ reduced density matrix for A as $CC^\dagger$ (also known as Schmidt eigenvalues). Referring them as $\lambda_1, \ldots, \lambda_N$, for example, the von-Neumann entropy is defined as $S = -\mathrm{Tr}\rho_A \ \log\rho_A = -\sum_n \lambda_n \ \log\lambda_n$ and $R_\alpha = \frac{1}{1-\alpha}\ln \mathrm{Tr}(\rho_A)^\alpha = \frac{1}{1-\alpha}\ln \sum_n \lambda_n^\alpha$.

A determination of the Schmidt eigenvalues requires a prior information about the state matrix C, i.e., the components of $|\Psi\rangle$ in a bipartite basis. The latter can in principle be obtained by solving the eigenvalue equation $H |\Psi\rangle = \lambda |\Psi\rangle$ with H. This in turn requires the determination of the matrix elements of the many-body Hamiltonian in the basis. But, as mentioned in section I, the error associated with exact determination of the matrix elements, further complicated by the fluctuating system conditions, render it necessary to describe the matrix elements by a statistical distribution in a physically motivated basis, e.g., the bipartite basis in the present case. Due to technical complexity of our theoretical ideas, it is helpful to first consider two prototypical examples.

(i) Quantum random energy model (QREM): We consider a one dimensional lattice of L spin $1/2$ particles in a random magnetic field, described by the Hamiltonian

$$H = H_{REM} + \Gamma \sum_{i=1}^{L} \sigma_i^x, \tag{1}$$

where, $H_{REM} = \sum_k E_k |k\rangle\langle k|$ is the random energy part of the Hamiltonian, diagonal in the S_z basis $\{|k\rangle\}$, such that the energies $\{E_k\}$ are independent and identically distributed as

$$P(E_k; h, L) = \frac{1}{\sqrt{\pi L}} e^{-\frac{E^2}{L}}, \tag{2}$$

and σ_x is one of the Pauli matrices which is the quantum part of the Hamiltonian. When Γ is a (negative) constant, eq. (1) becomes the well studied QREM [11–14].

For a fixed energy density e.g. $\epsilon = 0$, the dynamics of QREM is governed by the parameter transverse-field Γ. In the matrix space, however, this leads to a mere translation of the off-diagonal elements and there is an absence of diffusion. This is true in general when the variance of all the matrix elements are kept fixed.

In order to analyze the complexity-parameter formalism for this model, we consider Γ to be a basis-dependent random variable, such that,

$$\langle \delta\Gamma_{kl}^2 \rangle = \frac{1}{1 + (\frac{k-l}{b})^2}; \qquad \langle \Gamma_{kl} \rangle = 0, \tag{3}$$

i.e., with mean zero, and a power-law decaying variance. For $b = 0$ the variance of the off-diagonal elements vanishes and the system is classical (Poissonian), as is the case for $\Gamma = 0$. Whilst as $b \to \infty$ the system goes to the GOE limit, as is the case for large Γ.

For a matrix representation of H, we choose the product state basis spanned by 2^L vectors of type $|\mu\rangle \equiv \prod_{k=1}^{L} |m_k\rangle$ with each $\sigma_z|m_k\rangle = \pm|m_k\rangle$. A state Ψ of H in this basis can be expressed as $|\Psi\rangle \equiv \sum_{\mu} \psi_{\mu}|\mu\rangle$. For the entanglement analysis, we consider a bi-partition of the spin-chain into two equal subparts, referring them as subsystem A and B with their local basis spaces as $|a_{\mu}\rangle$ and $|b_{\mu}\rangle$. The basis state $|\mu\rangle$ can then be written as the $|\mu\rangle \equiv |a_{\mu} b_{\mu}\rangle$. The components of $|\Psi\rangle$ can now be written $C_{a_{\mu} b_{\mu}}$: $\psi_{\mu} \equiv C_{a_{\mu} b_{\mu}} \equiv \langle a_{\mu} b_{\mu}|\Psi\rangle$.

In the σ_z basis, the non-zero off-diagonal elements correspond to the basis which are at a Hamming distance one from the diagonal; this is because σ_i^x flips the spin at only one site i. Thus, there are L non-zero off-diagonal elements per line in the Hamiltonian eq. (1), and they are distributed independently according to the eq. (3). Further, considering the distribution of the diagonal elements as per eq. (2), we can write down the JPDF of the matrix elements of eq. (1) as

$$\rho_1(H) \propto \prod_{k} \exp\left(-\frac{H_{kk}^2}{L}\right) \prod_{\langle k,l \rangle} \exp\left[-\left(1 + \left(\frac{k-l}{b}\right)^2\right)\frac{H_{kl}^2}{2}\right], \tag{4}$$

where, $\prod_{\langle k,l \rangle}$ implies product over basis elements k and l which are at a Hamming distance 1 from each other.

(ii) One body Hamiltonian with Disorder (Anderson Model): Consider a single electron moving in d-dimensional disordered lattice. Within tight-binding approximation, the dynamics can be described by the Hamiltonian [15–18]

$$H = \sum_{\nu} \epsilon_{\nu}|\nu\rangle\langle\nu| + \sum_{\langle\mu,\nu\rangle} t_{\mu\nu}|\nu\rangle\langle\mu|. \tag{5}$$

with $t_{\mu\nu} = \langle\nu|t|\mu\rangle$ describes the tunneling amplitude of an electron between sites ν and μ, and the summation $\sum_{\langle\mu,\nu\rangle}$ is over z neighboring sites. Based on nature of the disorder,

the ensemble representing H can be of various types. For example, for the site-energies $H_{\nu\nu} = \epsilon_{\nu}$ as independent Gaussian distributions, $\rho_{\nu\nu}(H_{\nu\nu}) = \mathrm{e}^{-(H_{\nu\nu} - b_{\nu\nu})^2 / 2h_{\nu\nu}}$ with variance $h_{\nu\nu}$ and mean $b_{\nu\nu}$. The hopping can be chosen to be isotropic or anisotropic, non-random or random (Gaussian). A general form of the probability density $\rho(H) \equiv \prod_{\langle\mu,\nu\rangle} \rho_{\nu\mu}(H_{\nu\mu})$ of the ensemble, including all the above possibilities, can therefore be given as

$$\rho_2(H) = C \prod_{\mu} \exp\left[-\frac{(H_{\mu\mu} - b_{\mu\mu})^2}{v_{\mu\mu}}\right] \prod_{\langle\mu,\nu\rangle} \exp\left[-\frac{(H_{\mu\nu} - b_{\mu\nu})^2}{v_{\mu\nu}}\right], \qquad (6)$$

with C as a normalization constant, $\prod_{\langle\mu,\nu\rangle}$ imply product over connected sites only (depends upon number of neighbors), and $v_{\mu\nu} = 0 \, (\neq 0)$ for non-random (random) hopping.

III. VARIATION OF SYSTEM PARAMETERS: DIFFUSION OF ENSEMBLE DENSITY

Our prime interest in this work is to study the bipartite entanglement dynamics of an eigenstate of a many-body and one-body Hamiltonian H. A change in system conditions results in a variation of matrix elements of H and thereby its ensemble density which in turn manifests on the eigenfunction components in the basis space and their statistical behavior.

We note, while the matrix space for H an $\mathcal{N}$ dimensional space, the ensemble space for $\rho(H)$ is an $\mathcal{M}$ dimensional space consisting of independent ensemble parameters $v_{\mu\nu}$, and $b_{\mu\nu}$ with each point representing the state of the ensemble. Further, for $\rho(H)$ to be an appropriate representation of the statistical behaviour of H, $v_{\mu\nu}$ and $b_{\mu\nu}$ must depend on the system parameters, e.g., w, w_1, t, etc., as well as the physical dimensions of the system. Note the latter manifests in the matrix structure through its sparsity if the connectivity of the basis states through H is not uniform. Indeed, whether an element $H_{\mu\nu}$ is a nearest neighbour depends on the physical dimension of the system as well as on the boundary conditions which in turn affects the number of non-zero elements. As discussed in [19], a change in system conditions can subject the matrix elements $H_{\mu\nu}$ to undergo a Langevin dynamics, resulting in diffusion of $\rho(H)$ in matrix space with finite drift; here the noise originates from the lack of accuracy in the estimation of $H_{\mu\nu}$ and finite drift from the physical constraints on the dynamics. But as the ensemble parameters are functions of system parameters, they also vary, leading to an evolution of $\rho(H)$ in the ensemble space too. For the evolving ensemble to continue representing the system, it is desirable that the evolution of $\rho(H)$ in

matrix space is exactly mimicked by that in the ensemble space. As discussed in previous studies [20–23], a specific combination of first order variation of the ensemble parameters $v_{\mu\nu;s} \to v_{\mu\nu;s} + \delta v_{\mu\nu;s}$ and $b_{\mu\nu;s} \to b_{\mu\nu;s} + \delta b_{\mu\nu;s}$ over time would lead to a Brownian dynamics in Hermitian matrix space (introduced by Dyson for Hermitian case and discussed in detail, e.g., in [24–26]), starting from an arbitrary initial condition and with a stationary ensemble as the equilibrium limit. A transformation of the set $\{v_{\mu\nu}, b_{\mu\nu}\}$ to another set $\{t_1, t_2, \ldots, t_M\}$ however reduces the multi-parametric dynamics in the ensemble space to a single parameter dynamics, say with respect to t_1, while others, i.e, $t_2 \ldots t_M$ remaining constant throughout the evolution,

$$\frac{\partial \rho}{\partial t_1} = L\,\rho; \qquad \frac{\partial \rho}{\partial t_\alpha} = 0, \quad \alpha > 1 \tag{7}$$

where,

$$L \equiv \sum_{\mu,\nu} \frac{\partial}{\partial H_{\mu\nu;s}} \left[\frac{g_{\mu\nu}}{2} \frac{\partial}{\partial H_{\mu\nu;s}} + \gamma H_{\mu\nu;s} \right] \tag{8}$$

with $g_{\mu\nu} = 2$ or 1 for $\mu = \nu$ and $\mu \neq \nu$, respectively, and

$$t_1 = -\frac{1}{2M\gamma} \ln \left[\prod_{s=1}^{\beta} \prod_{\mu \leq \nu} |g_{\mu\nu} - 2\gamma v_{\mu\nu;s}| \, |b_{\mu\nu;s}|^2 \right] + const. \tag{9}$$

To distinguish t_1 from $t_2, \ldots, t_M$, hereafter we replace t_1 by Y. The product in eq. 9 is over M non-zero terms. As clear from the above, Y turns out to be an average distribution parameter, a measure of average uncertainty of system, also referred as the ensemble *complexity parameter*. As examples, here we give $Y - Y_0$, where Y_0 correspond to the initial complexity parameter, for the Hamiltonian H (eq.(1)) and (eq.(3)) with $\rho(H)$ given by eq.(4). Choosing localized phase as the initial condition ($b = 0$), and using eqs. eq.(4) and (3) in eq.(9) gives

$$Y - Y_0 = -\frac{1}{2(N+1)\gamma} \sum_{r=0}^{L-1} \ln \left| 1 - \frac{2\gamma}{1 + (\frac{2^r}{b})^2} \right|. \tag{10}$$

The summation above corresponds to the fact that a Hamming distance 1 between the basis elements $|k\rangle$ and $|l\rangle$ correspond to the distance $|k - l| = 2^r$ in the matrix space, with $r = 0 \cdots L - 1$.

Similarly, for the Anderson model, eq. (5),

$$Y = -\frac{N}{2M\gamma}\alpha + C_0, \tag{11}$$

where,

$$\alpha = \ln|1 - \gamma w^2| + (z/2)\ln[|1 - 2\gamma w_1^2||t + \delta_{t,0}|^2], \tag{12}$$

and, $M = \frac{N}{2}[N + z(1 - \delta_{t,0}) + 1]$. Here, we have taken an isotropic hopping with mean t. We choose the initial condition to be the localized phase, such that $w = w_m \gg 1/$ Thus, we have,

$$Y - Y_0 = -\frac{N}{2M\gamma}\ln\left|\frac{1 - \gamma w^2}{1 - \gamma w_m^2}\right|. \tag{13}$$

Also, γ is related to the variance of the matrix elements in the ergodic limit. More precisely, in our numerical calculations, we choose $\gamma = \frac{1}{2w_0^2}$, where w_0 is the smallest value of w we take in the Anderson model, and $\gamma = 1/2$ for the QREM.

IV. EVOLUTION OF SCHMIDT EIGENVALUES WITH SYSTEM PARAMETERS

An eigenfunction Ψ of the Hamiltonian H can in principle be obtained by solving the eigenvalue equation $H\Psi = \lambda\Psi$. Contrary to the eigenvalues, however the behavior of eigenfunctions depend on the basis in which the latter is represented. The study [10] describes the complexity parameter based evolution of the eigenfunction statistics in an arbitrary basis. For studying bipartite entanglement analysis, however, we require a bipartite basis. Here we give the necessary steps rewriting the evolution equation in an arbitrary basis to a bipartite one.

A. Evolution equation for the eigenfunction components

As discussed in detail in the supplementary material, eq. (7) can further be used to derive the Y governed evolution of the JPDF P_ψ of the components of an eigenfunction $\Psi = \sum C_{kl}|a_k b_l\rangle$ in a bipartite basis. The evolution equation can be given as

$$\frac{\partial P_\psi}{\partial Y} = \frac{\beta^2 \chi_0}{4\Delta_{local}^2} \sum_{m,k} (L_{mk} + L_{mk}^*) P_\psi \tag{14}$$

with $L_{mk} \equiv \frac{\partial}{\partial C_{mk}}\left(\sum_{n,l} \frac{\partial(\delta_{mn}\delta_{nl} - C_{mk}C_{nl}^*)}{\partial C_{nl}^*} + (N-1)C_{ml}\right)$ and Δ_{local} as the local mean level spacing.

We emphasize that, contrary to previous studies, eq. (14) is derived directly from the Hamiltonian matrix ensemble for a complex system and is therefore more realistic. Indeed, an evolution equation for the state matrix components was derived in [7] directly by invoking maximum entropy hypothesis to determine the distribution of the components of an arbitrary quantum state in a bipartite basis; the equation can again be written in the form of eq.(14) but with $L_{mk} \equiv \frac{\partial}{\partial C_{mk}} \left(\frac{\partial}{\partial C_{mk}} + C_{mk} \right)$.

B.   Moments for Reduced Density Matrix

With diffusive dynamics of the matrix elements C_{kl} expected to manifest itself in the reduced density matrix space W, the moments for the matrix elements $W_{mn} = \sum_{k=1}^{N_A} C_{mk} C_{nk}^*$ can be calculated from those of C. As discussed in Appendix B, a comparison of eq. (14) with standard Fokker-Planck equation gives

$$\langle \delta C_{mn} \rangle = -\frac{\beta \chi_0 (N-1)}{2 \Delta_{local}^2} C_{mn} \, \delta Y \tag{15}$$

$$\langle \delta C_{mn} \, \delta C_{kl}^* \rangle = \frac{\beta \chi_0}{\Delta_{local}^2} (\delta_{mk} \delta_{nl} - C_{mn} C_{kl}^*) \, \delta Y \tag{16}$$

The above relations lead to following moments (discussed in more detail in Appendix C):

$$\langle \delta W_{mm} \rangle = -\beta (N-1) W_{mm} \delta \Lambda. \tag{17}$$

$$\langle \delta W_{mn} \, \delta W_{mn}^* \rangle = [\beta (W_{mm} + W_{nn}) - 4 W_{mm} W_{nn}] \, \delta \Lambda \tag{18}$$

$$\langle \delta W_{mm} \, \delta W_{nn} \rangle = -4 \, W_{mm} W_{nn} \, \delta \Lambda \tag{19}$$

where Λ is the rescaled evolution parameter

$$\Lambda = \chi_0 (Y - Y_0) R_{local}^2, \tag{20}$$

with $R_{local} = \frac{\xi^d}{\Delta_e N}$ as the local mean level density, ξ as the localization length, d as the physical dimension of the system, Δ_e as the local mean level spacing with Y_0 corresponding to initial value of Y (i.e. for the initial state of evolution).

C.   Evolution equation for Schmidt eigenvalues

As the fluctuations of eigenfunction components are expected to manifest through those of the ρ_A matrix elements on the Schmidt eigenvalues $\{\lambda_i\}$, next we seek the JPDF $P(\lambda) \equiv$

$P(\{\lambda_i\}) \equiv P(\lambda_1, \ldots, \lambda_{N_A})$ and its evolution under changing system conditions. This can be derived using the standard second-order perturbation theory along with eqs. (17)-(19); under Markovian dynamics assumption, only the moments up to first order in δY are needed. As discussed in detail in Appendix C, the evolution equation for $P(\{\lambda_i\})$ turns out to be

$$\frac{\partial P}{\partial \Lambda} = \mathcal{L}P - \sum_{m,n=1}^{N_A} \frac{\partial^2}{\partial \lambda_n \lambda_m} [(\lambda_n \lambda_m)P] \tag{21}$$

where

$$\mathcal{L} \equiv \sum_{n=1}^{N_A} \left[\frac{\partial^2 (\lambda_n\, P)}{\partial \lambda_n^2} - \beta \frac{\partial}{\partial \lambda_n} \left(\sum_{\substack{m=1 \\ m \neq n}}^{N_A} \frac{\lambda_n}{\lambda_n - \lambda_m} + \nu - \eta \lambda_n \right) \right] \tag{22}$$

with $\eta = \frac{N}{2}$ and $\nu = \frac{N_A - N_B - 1}{2}$.

We note that the above equation is similar to the one derived in previous work [7]. Nevertheless, there are crucial differences, basically reflecting the effect of correlations among eigenfunction components present in a quantum state; this aspect was ignored in the previous works [7–9].

V.   EVOLUTION OF INFORMATION ENTROPIES

Following similar steps as described in [7], the diffusion equation of entanglement measures from eq. (21), is straight forward to calculate, which is similar to as obtained in [7–9]. However, a crucial difference from previous works is that the condition $\text{Tr}\rho = 1$ is already implemented and is inherent in P_ψ (as the eigenfunction is normalized from the beginning), this simplifies the calculations substantially. Another important difference is the second term on the right side of eq. (21). (The details of the calculations in this section are give in the supplementary material.)

The von Neumann entropy $R_1 = -\sum_n \lambda_n \log \lambda_n$ is a standard measure to quantify the bipartite entanglement of pure states. Its ensemble average can be defined as

$$\langle R_1 \rangle = \int \left(-\sum_n \lambda_n \log \lambda_n \right) P_\lambda(\lambda)\, \mathrm{D}\lambda. \tag{23}$$

Differentiating the above equation with respect to Λ, followed by substitution of eq.(21) and simplifying by partial integration, we have

$$\frac{\partial \langle R_1 \rangle}{\partial \Lambda} = -(N_A^2 - 1) + \frac{N}{2} + N_A \nu + \frac{N_B}{2} \langle R_0 \rangle - \frac{N}{2} \langle R_1 \rangle. \tag{24}$$

12

The above equation describes the Λ-governed evolution for the average R_1 and its solution for arbitrary Λ can be given as

$$\langle R_1 \rangle(\Lambda) = R_{1,\infty}(1 - e^{-\frac{N\Lambda}{2}}), \tag{25}$$

In limit $\Lambda \to \infty$, with $\langle R_0 \rangle \to N_A \log N_A + \frac{N_A^2}{2N_B}$ [7], eq.(25) gives $\langle R_1 \rangle \to R_{1,\infty} \approx \log N_A - \frac{N_A}{2N_B}$. The latter agrees with the Page limit [27] for the ergodic states; (we recall that the state Ψ approaches ergodic limit as $\Lambda \to \infty$).

Proceeding along the same route, we also derive the Λ governed evolution of the variance of the von Neumann entropy, defined as $\langle \delta R_1^2 \rangle = \langle R_1^2 \rangle - \langle R_1 \rangle^2$; the details are discussed in the supplementary material. The evolution equation of the variance can be given as

$$\frac{\partial \langle \delta R_1^2 \rangle}{\partial \Lambda} = 2(Q - \langle R_1^2 \rangle) + N_B \operatorname{cov}(R_0, R_1) - N \langle \delta R_1^2 \rangle \tag{26}$$

where, the covariance $\operatorname{cov}(R_0, R_1) \equiv \langle R_0 R_1 \rangle - \langle R_0 \rangle \langle R_1 \rangle$, and $Q \equiv \left\langle \sum_n \lambda_n (\log \lambda_n)^2 \right\rangle$. While we cannot solve eq. (26) as the first two terms on the right-hand side (RHS) are analytically intractable, we can perform the following analysis. At first, we can try to analyze the ergodic limit, $\Lambda \to \infty$, when the RHS of the eq. (26) goes to zero. As indicated by the fig. 1, the $\operatorname{cov}(R_0, R_1)$ in that limit is vanishing, while the first term on the RHS is positive and $\mathcal{O}(1)$. This implies that $\langle \delta R_1^2 \rangle \sim \frac{1}{N}$ in the ergodic limit; as already indicated in the previous studies [2, 9, 28].

Away from the ergodic limit, the RHS of eq. (26) is dominated by the covariance term. The negative sign of the covariance is expected as $\langle R_0 \rangle$ decreases from $\infty \to N_A \log N_A$, while $\langle R_1 \rangle$ increases from $0 \to \log N$ as the system transitions from a localized $\to$ ergodic regime. More interestingly, the divergence of the covariance is akin to that of the $\langle \delta R_1^2 \rangle$; in fact, the behavior of $|\operatorname{cov}(R_0, R_1)|$ is qualitatively the same as the latter (fig. 1).

Another way to quantify entanglement is through the purity of the reduced density matrix, defined as $S_2(\lambda) = \sum_n \lambda_n^2$. Its ensemble average can be defined as

$$\langle S_2 \rangle = \int \left(\sum_{n=1}^{N_A} \lambda_n^2 \right) P(\lambda) \, \mathrm{D}\lambda \tag{27}$$

Proceeding similar to the calculation for R_1, we get,

$$\frac{\partial \langle S_2 \rangle}{\partial \Lambda} = a - b \langle S_2 \rangle; \qquad a = N_A + N_B + 1, \ b = N + 2, \tag{28}$$

$$\frac{\partial \langle \delta S_2^2 \rangle}{\partial \Lambda} = -2 b \langle \delta S_2^2 \rangle + 8 \langle S_3 \rangle, \tag{29}$$
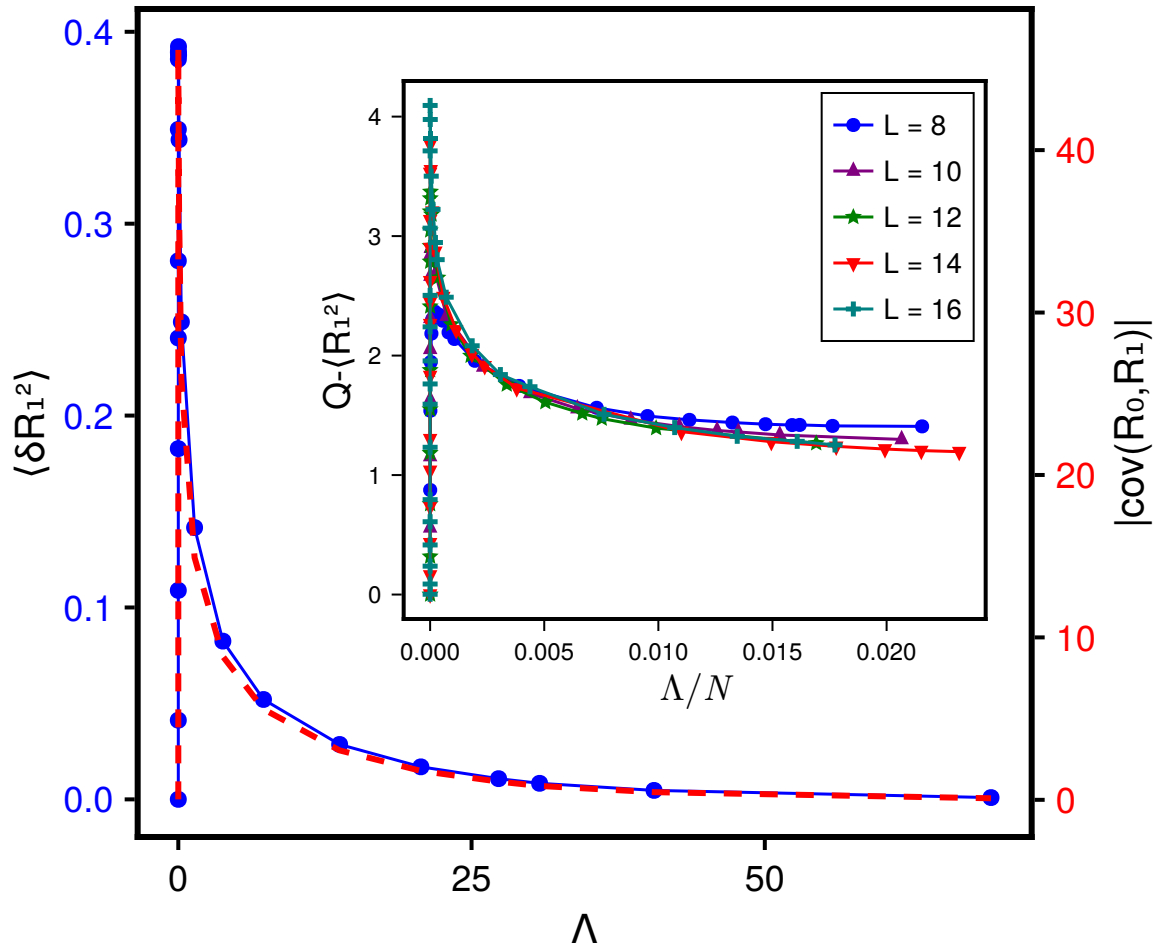
FIG. 1: **Analysis of the RHS of the eq.** (26). We compare the $|\text{cov}(R_0, R_1)|$ (red dashed line) and the $\langle \delta R_1^2 \rangle$ for $L = 12$. As can be seen, the quantities are qualitatively quite similar, and that in the ergodic regime the former tend to zero. This gives us the intuition that the diverging variance of R_1 is, in fact, a consequence of the diverging covariance $\text{cov}(R_0, R_1)$. (inset) We show the dynamics of $Q - \langle R_1^2 \rangle$, which is also diverging but $\mathcal{O}(1)$ for all system sizes, and hence dominated by the covariance term.

With the initial conditions $\langle S_2 \rangle (\Lambda = 0) = 1$, and $\langle \delta S_2^2 \rangle (\Lambda = 0) = 0$, the solution of the above equations turns out to be

$$\langle S_2 \rangle (\Lambda) = \frac{a}{b} + \frac{b-a}{b} e^{-b\Lambda}, \tag{30}$$

14

and,

$$\langle \delta S_2^2 \rangle (\Lambda) = \frac{4}{b^3} \left[6(ab - a^2)e^{-\frac{b\Lambda}{2}} + 4(2a^2 + b^2 - b - 3ab)e^{-\frac{3b\Lambda}{2}} - (3a^2 - 6ab + 4b^2 - 3b)e^{-2b\Lambda} + a^2 + b \right]. \tag{31}$$

The latter can be simplified for the balanced case, i.e., $N_A = N_B = D$

$$\langle \delta S_2^2 \rangle (\Lambda) = \left(\frac{1}{D^4} \right) \left(20 - 4(3 - 2D)^2 e^{-2D^2\Lambda} + 48(D - 2) e^{-D^2\Lambda} + 16(7 + D(D - 6)) e^{-\frac{3D^2\Lambda}{2}} \right). \tag{32}$$

In the ergodic limit the $\langle S_2 \rangle$ saturates to the expected value $\frac{a}{b} \approx \frac{N_A + N_B}{N}$. Comparing eqs. (30) and (25), one can note that while $\langle R_1 \rangle$ exponentially increases before saturating in the ergodic limit, the $\langle S_2 \rangle$ decreases exponentially before saturating. However, the crucial difference is that the latter reaches the steady state twice as fast the R_1, as can be deduced comparing the arguments of the exponential in the two equations.

Moreover, the eq. (32) shows the expected behavior of the variance: starting from zero in the separable regime, it reaches a maximum at a point which can be taken as a proxy for the phase transition point [29], and then decays saturating to the ergodic limit which is $\sim \frac{1}{D^4}$ [2, 9]. Moreover, we note from eq. (29) that the variance of purity depends on higher order moment $S_3 \equiv \sum_n \lambda_n^3$. Fortunately, the latter can be derived from eq. (21) in closed form, which can be further used to obtain the solution of eq. (29).

VI. EVOLUTION OF THE SINGLE-PARTICLE ENTANGLEMENT ENTROPY (SPEE)

The single-particle entanglement entropy (SPEE) can then be defined as [17, 18]

$$S_A(\rho_A) = -P_A \log P_A - (1 - P_A) \log(1 - P_A), \tag{33}$$

where, $P_A \equiv \sum_{r \in A} |\psi(r)|^2$. A and B are the two bi-partitions, created, for example, by slicing the 3D lattice horizontally. The entanglement can then be understood to be between the two modes wherein the particle occupies either the part A or B of the lattice. In the ergodic limit, for a balanced bi-partition, $P_A \to 0.5$ and hence $S_A \to \log(2)$. Consequently, $S_A \in [0, \log(2)]$.

The evolution equation for the S_A turns out to be (details in the supplementary material)

$$\frac{\partial \langle S_A \rangle}{\partial \Lambda} = -4 - 2N \langle S_A \rangle - N \langle \log P_A P_B \rangle. \tag{34}$$

At first, we can note that, as $\Lambda \to \infty$, $P_A = P_B = 1/2$. Consequently, $\langle S_A \rangle_\infty = \log 2 - \frac{2}{N}$. However, determining $\langle \log P_A P_B \rangle$ turns out to be quite complicated, for it in turn depends upon the knowledge about $\langle (P_A P_B)^{-1} \rangle$. In general, we can deduce,

$$\frac{\partial \langle (P_A P_B)^k \rangle}{\partial \Lambda} = k[4(k-1) + N] \langle (P_A P_B)^{k-1} \rangle - 4k(N + 4k - 2) \langle (P_A P_B)^k \rangle, \tag{35}$$

i.e., $\langle (P_A P_B)^{-1} \rangle$ requires knowledge about $\langle (P_A P_B)^{-2} \rangle$, and so on. Because of this, understanding the evolution of $\langle \log P_A P_B \rangle$, and hence of $\langle S_A \rangle$, is analytically infeasible. Nevertheless, we would like to point out that $-\langle \log P_A P_B \rangle$ goes from $\log 4$ (ergodic) to ∞ (localized) and is similar to the $\langle R_0 \rangle$ in eq. (24), but with one crucial difference: unlike $\langle R_0 \rangle$, the former isn't extensive in sub-system size N_A, and can't be assumed constant in the limit $N_A \to \infty$.

From eq. (35) we can obtain,

$$\langle P_A P_B \rangle = \frac{N}{4(N+2)} \left[1 - e^{-4(N+2)\Lambda} \right], \tag{36}$$

and,

$$\langle \delta (P_A P_B)^2 \rangle = \frac{1}{16N^3} \left[8N + 8N(N+4)e^{-4(N+2)\Lambda} - N(N^2 + 16N)e^{-8(N+2)\Lambda} + N(N^2 + 8N)e^{-8(N+6)\Lambda} \right] \tag{37}$$

Quite interestingly, in the ergodic limit, $\langle \delta (P_A P_B)^2 \rangle \sim \frac{1}{N^2}$. That is, unlike the $\langle P_A P_B \rangle$, the $\langle \delta (P_A P_B)^2 \rangle$ in the ergodic limit depends upon the system size and is similar to that of purity studied in the previous section.

The eqs. (36) and (37) are compared with the exact diagonalization results for a system of size $L = 18$ in fig. 2. While there is good agreement between the theoretical and the numerical results of the average behavior, the theory shows a faster evolution of the variance as compared to the numerics. However, we expect that the agreement for the variance can be improved by diagonalizing larger systems.

VII. NUMERICAL ANALYSIS

A numerical study of the entanglement entropy for engineered non-ergodic states with complex coefficients and its complexity parametric dependence is discussed in [7]. In the present analysis of the Hamiltonian eq. (1), the states consist of real coefficients only.
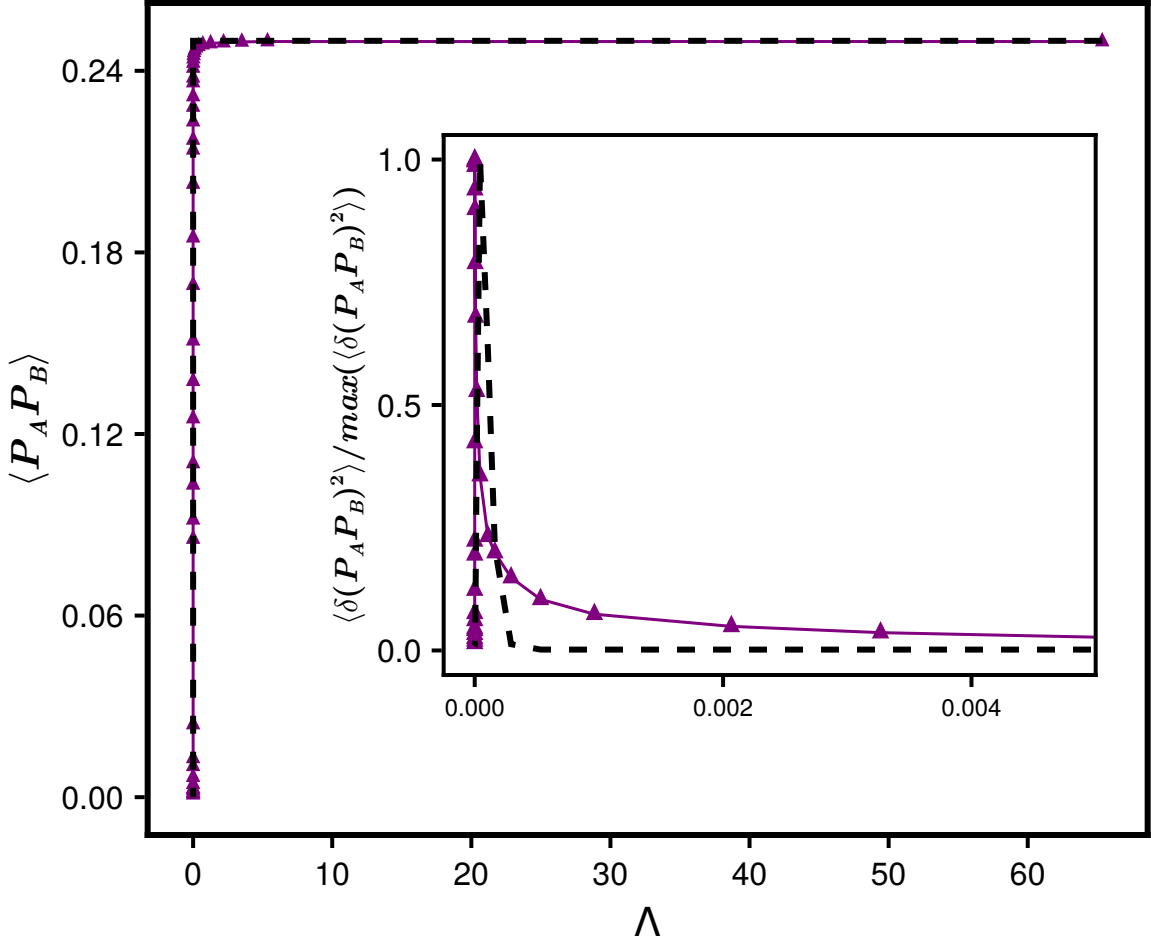
16

FIG. 2: **Dynamics of $P_A P_B$.** We show the evolution of the $\langle P_A P_B \rangle$, and (inset) $\langle \delta (P_A P_B)^2 \rangle$ for the 3D Anderson Hamiltonian of size $L = 18$. The theoretical formulas eqs. (36) and (37) is also shown (black dashed line) to compare with the exact diagonalization results.

A. QREM

We exactly diagonalize the Hamiltonian in eq. (1) for several system sizes L. For each L, we diagonalize the system for several values of the parameter b in eq. (3) ranging from 0, corresponding to a localized state, to a sufficiently large value such that the system reaches to the ergodic regime. Moreover, in this work, we have focused on the entanglement properties of the eigenstates in the bulk of the spectrum, i.e., at $E = 0$, for which we use the standard *shift-invert* diagonalization technique to calculate 1% of the total eigenpairs at $E = 0$ [30]. We would like to emphasize here that since the complexity parameter Λ is energy dependent, we take a small fraction (1%) of eigenpairs to make sure that the Λ we

calculate is indeed for $E = 0$. For an efficient implementation of the *shift-invert* technique and efficient computation for large systems leveraging MPI techniques, we diagonalize the Hamiltonian using the SLEPc library in C [31].

We calculate the average entanglement and the fluctuation around the average over various disorder realizations and over about 1% of the total eigenstates per realization at $E = 0$. The Λ is calculated from the eq. (20) with $\xi^d = \langle I_2 \rangle^{-1}$, where I_2 is the inverse participation ratio (IPR) [32]. It was highlighted in ref. [10], that while the eigenvalue statistics depend only on Λ, the eigenvector statistics depend on both the Λ and the system size. Consequently, to compare the statistics of entanglement for various system sizes, we plot the average and the variance of R_1 with Λ/N in fig. 3. Furthermore, since the average entanglement in the ergodic limit and the peak value of the fluctuations is dependent on the system size, to wash out the finite-size effects we rescale the $\langle R_1 \rangle$ and the $\langle \delta R_1^2 \rangle$ by their maximum value. As can be seen in fig. 3, the curves for different system sizes start overlapping on top of each other for large system sizes. We also compare eq. (25) for $L = 16$ with the numerical results (the black dotted line), which doesn't seem to be a good match. We think this could be due to the fact that eq. (25) was obtained from eq. (24) for the limit $N_A \to \infty$.

The dynamics of purity of the reduced density matrix, S_2, with Λ/N is shown in fig. 4. Unlike the von Neumann entropy, S_2 isn't a measure of entanglement since it doesn't go to zero in the separable limit [33]. As a result, even with a rescaling of the y-axis the finite-size effects persist. A simple measure of entanglement related to S_2 is the linear entropy (LE) [34, 35]

$$S_L = 1 - S_2, \tag{38}$$

such that $S_L \in [0, \frac{N-1}{N}]$. We can now rescale S_L by its maximum value to get rid of the finite-size effects, ref. fig. 30. We have also compared the analytical results for the purity, eq. (30), in the fig. 4: we see that unlike the case of R_1 the matching of analytical results with numerics is rather good. This is due to the fact that no approximations regarding the system size are taken in obtaining the eq. (30). Moreover, as indicated in the previous section, the purity and the linear entropy reaches the steady state faster than the von Neumann entropy.
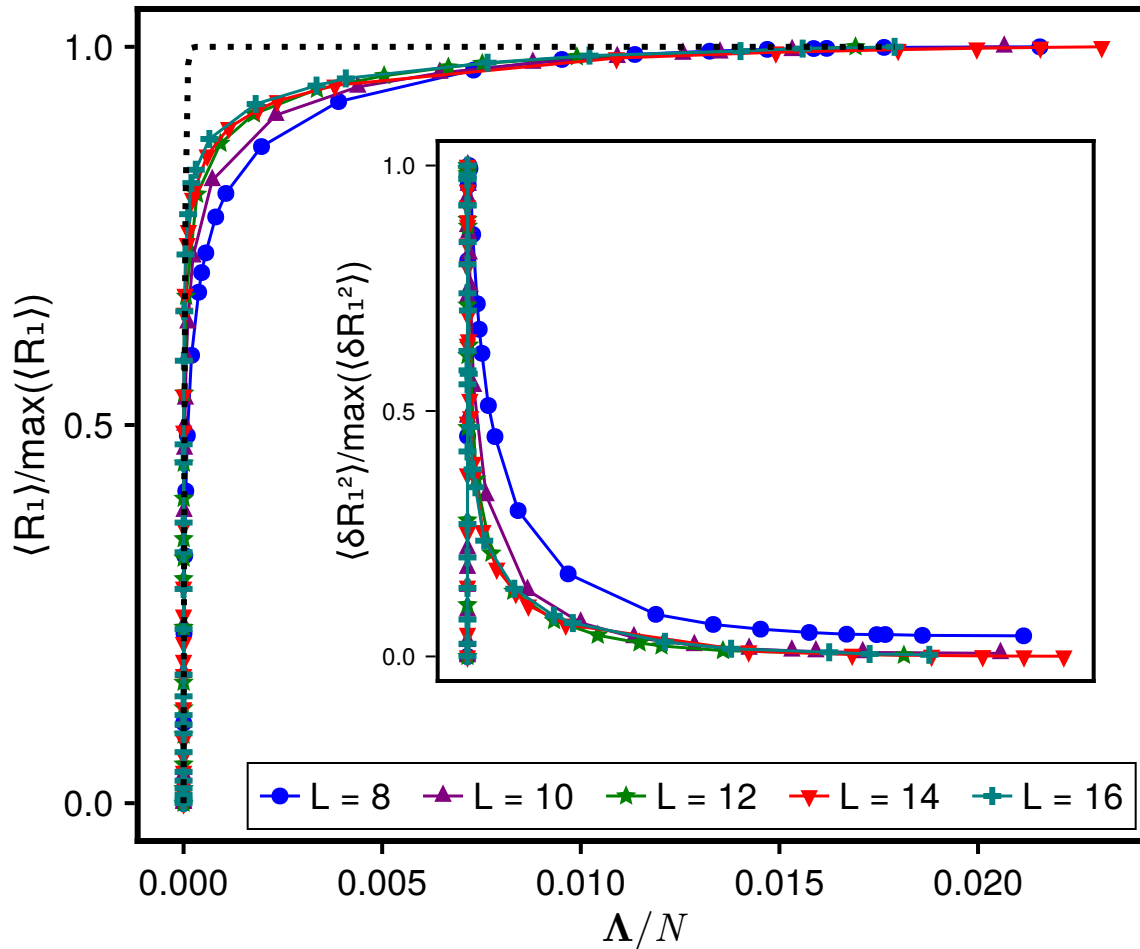
FIG. 3: **Average and variance of von Neumann Entropy in the QREM.** The dynamics of the average and (inset) variance of the von Neumann entropy R_1, for system sizes $L = 8, 10, 12, 14, 16$ over disorder realizations $2000, 1000, 500, 100, 10$ and $10, 10, 40, 500, 650$ eigenstates per realizations respectively, with Λ/N is shown. The y-axes have been rescaled by their maximum value to avoid finite-size effects. As can be seen, the curves for different system sizes overlap on top of each other for large L (> 10) when plotted with Λ/N. The analytical expression eq. (25) is also plotted (black dotted line) is also shown for $L = 16$. The latter, however, is obtained for the $N_A \to \infty$ limit, and hence is not a good match with the finite-size numerics.

B. 3D Anderson Model

We exactly diagonalize an $L \times L \times L$ three-dimensional Anderson Hamiltonian eq. 5 with periodic boundary condition for $L = 12$ for several diagonal disorder strength parameter w.
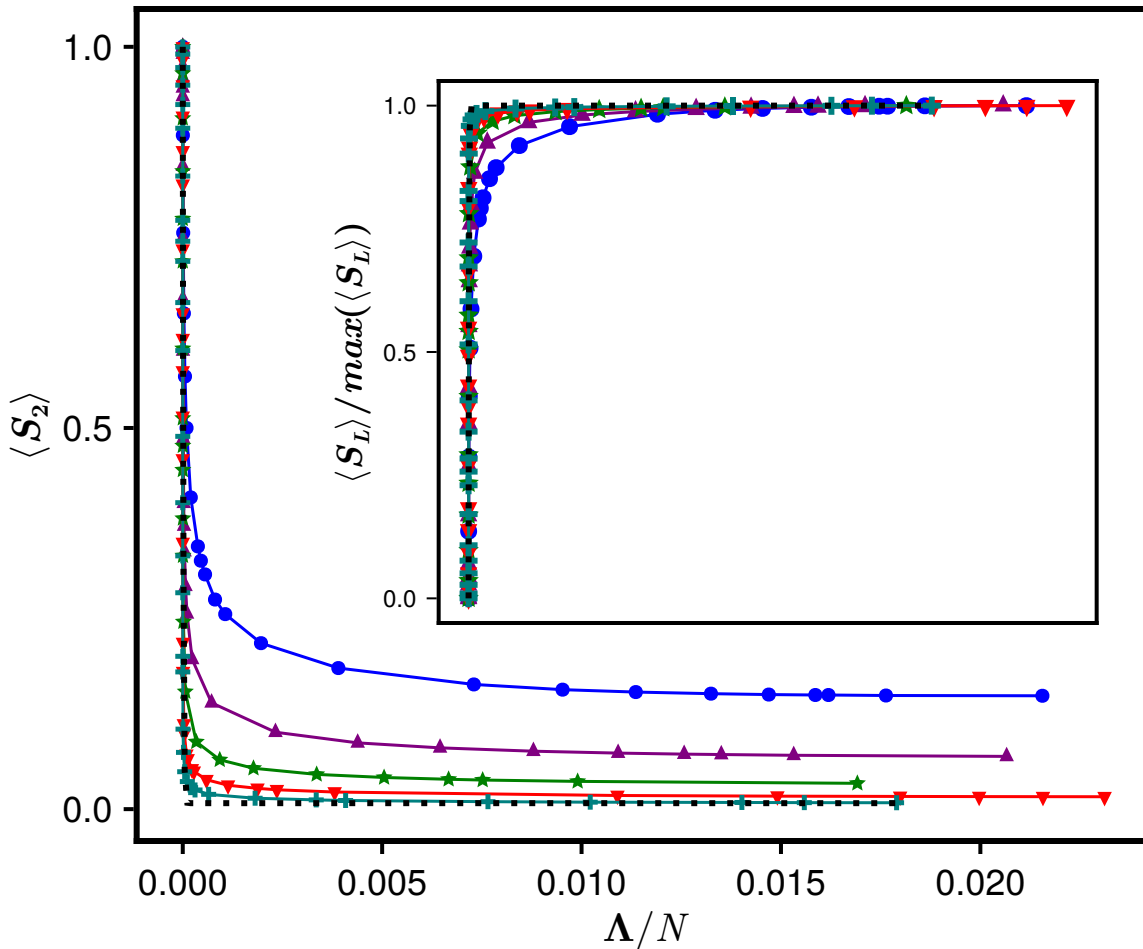
FIG. 4: **Average of purity and linear entropy in the QREM.** The dynamics of the average purity (S_2) and (inset) the linear entropy (S_L), over many disorder realizations and a fraction of eigenstates per realizations for various system sizes (details same as in fig. 3), with Λ/N is shown. In the ergodic limit, $S_2 \sim \frac{1}{N_A}$, as a result, the curves don't agree in the that limit, although the finite-size effects tend to decrease as system size increases. The theoretical prediction, eq. (30), seems to match well with the numerical data. (inset) The linear entropy, eq. (38), is shown with the y-axis rescaled by its maximum. Similar to R_1, the measure, rescaled by its maximum, is less sensitive to the finite-size effects, however, the approach to the steady state is comparatively faster; cf. fig. 3.

We consider several combinations of the various parameters involved in the Hamiltonian, viz., the off-diagonal hopping mean t and variance w_1, and the sparsity parameter k, such that $k = 1$ imply nearest neighbor interaction and $k = 2$ implying next nearest neighbor
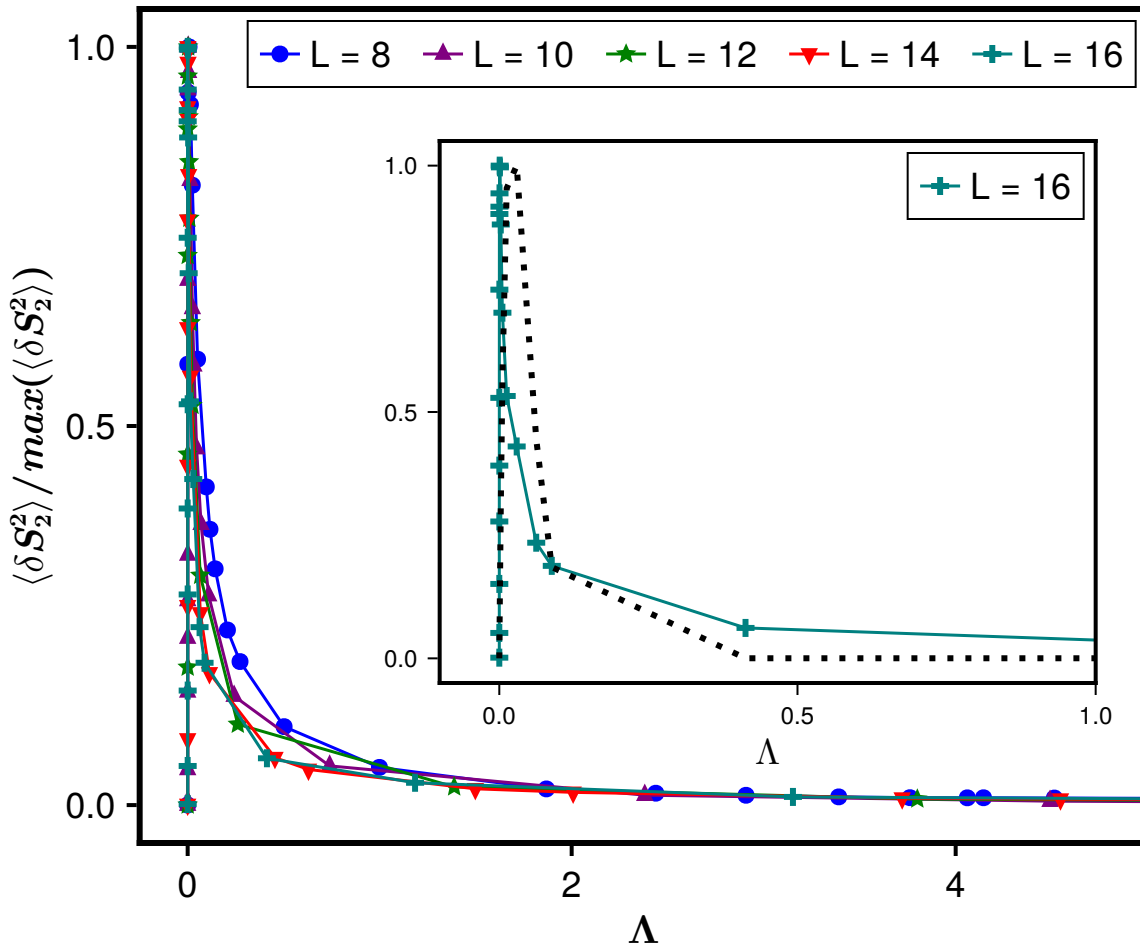
FIG. 5: **Variance of purity in the QREM.** The dynamics of the variance of purity (S_2) and (inset) its comparison with theory (black dotted line) eq. (32) for $L = 16$ is shown. As indicated earlier, eq. (32) varies rapidly with Λ, hence the complete dynamics is difficult to see for large L. Moreover, contrary to the variance of R_1, ref. inset of fig. 3, the collapse for different L seems better with Λ instead of Λ/N. We think this is because of different competing exponentials in eq. (32) cancelling the effect of system size. Furthermore, we find that the theory predicts a much faster decay of the variance than observed in the numerics. A comparison with the numerics is done after rescaling $\Lambda \to \Lambda/N^{0.7}$.

interaction. The sparsity, of course, is more in the former case with each site having $z = 6$ neighbors, while in the latter, each site has $z = 24$ neighbors. Throughout this analysis, we have kept t fixed to 0.5. For each set of parameters, we consider 1000 disorder realizations (except for $L = 18$ where we consider only 100 realizations) and obtain about 1% eigenpairs

at the energy $E = 0$.

The average and variance of the SPEE with Λ for various combinations of the parameters is shown in the figs. 6 and 7. For a comparison, the inset shows the dynamics with the diagonal disorder parameter w. As can be seen, the curves corresponding to system with nearest neighbor ($k = 1$) and next nearest neighbor interaction ($k = 2$) but same off-diagonal variances (w_1) shows single-parametric evolution. The slight difference between the dynamics with random ($w_1 = 1$) and non-random ($w_1 = 0$) hopping is attributed to the large difference in their Λ (ref. fig. 8): the Λ for non-random hopping is an order of magnitude larger than the Λ for the system with random hopping elements. Consequently, the latter evolves slightly faster. Also, we find that the dynamics of the statistics of $P_A P_B$ is qualitatively quite similar to that of the SPEE, and we have omitted its discussion because of repetition.

VIII.   CONCLUSION

In the end we summarize our main results and open questions. In this work, we have presented a theoretical analysis of the entanglement dynamics of the pure bipartite states of Hamiltonians with uncorrelated matrix elements as system conditions vary. Our analysis indicates the existence of a common mathematical formulation of the entanglement measures where system dependence appears collectively through a functional of the system parameters, Λ.

Due to the complexity of the system, with or without disorder, the matrix elements of its Hamiltonian are best described by their JPDF. A change in the system conditions leads to an evolution of the JPDF of the matrix elements, and in turn, an evolution of the JPDF of the eigenfunction components and the eigenvalues. The evolution of the latter with Λ was studied in detail in ref. [10]. Based on this, here, we have derived the evolution of the JPDF of the Schmidt eigenvalues, by writing the eigenfunction in a bipartite basis, which in turn yield the evolution equation of entanglement measures. For the SPEE, the evolution can be directly determined from the JPDF of the eigenfunction in the site basis.

For the many-body Hamiltonian, we have obtained the evolution equation for the average and the variance of the von Neumann entropy (R_1) and the purity (S_2). While the latter could be obtained without making any assumptions on the system size, the evolu-
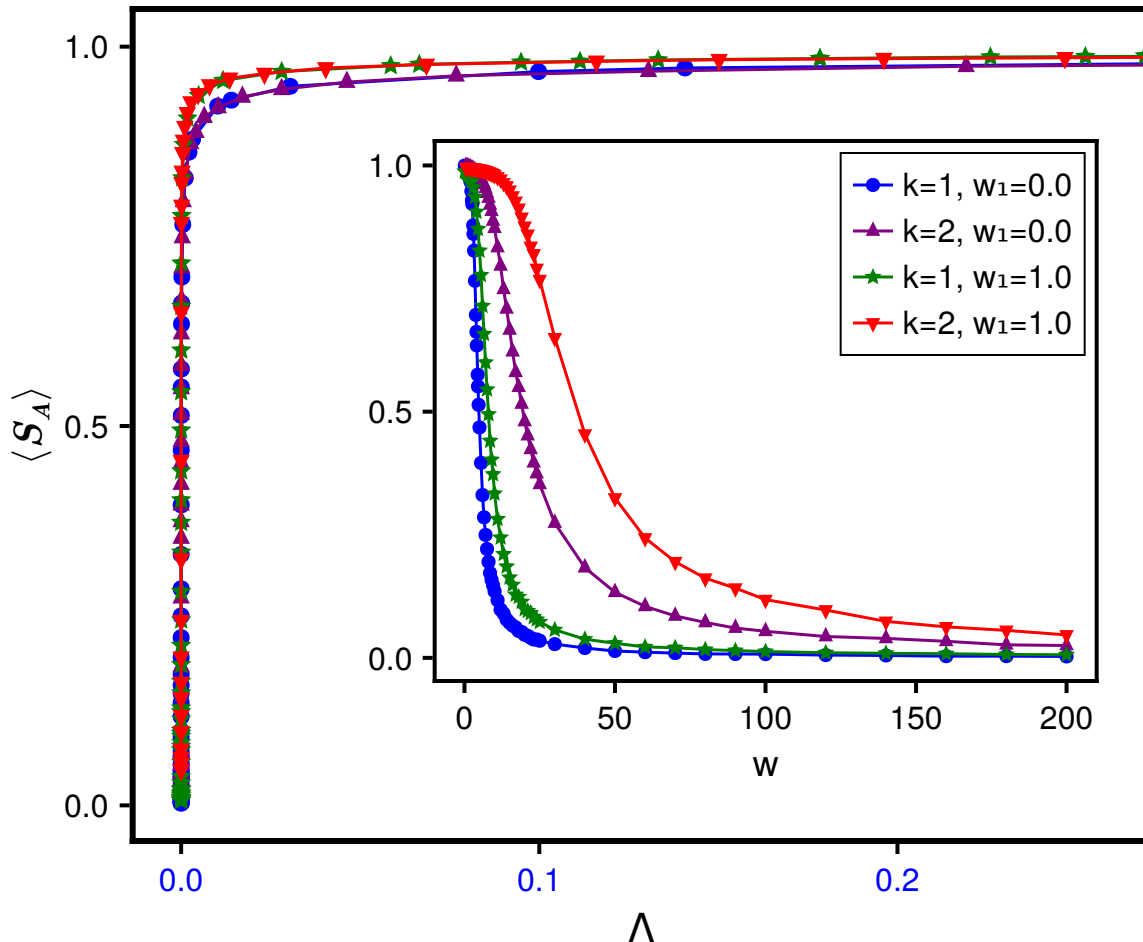
22

FIG. 6: **Evolution of average SPEE.** The evolution of the $\langle S_A \rangle$, eq. (33), for a cubic lattice of dimension $L = 12$ is shown for various combinations of the system parameters w_1 and k, while keeping $t = 0.5$ fixed for all the cases. In the inset, we show how for different choice of the parameters leads to distinguishing curves of evolution with the diagonal disorder parameter w. Nevertheless, with Λ they tend to show a single-parametric evolution for same w_1. The slight difference between the evolution of different w_1 is attributed to the large difference in their Λ (ref. fig. 8).

tion equation of the $\langle R_1 \rangle$ is obtained for large subsystem size, $N_A \to \infty$. An interesting corollary of this analysis is that $\langle S_2 \rangle$ evolves twice as fast as $\langle R_1 \rangle$, which is also supported by the numerical results. Moreover, we find that the fluctuation of entanglement measures are dependent upon other non-linear function(s) of the Schmidt eigenvalues, e.g., $\langle R_0 \rangle$ and $\langle S_3 \rangle$. In obtaining the evolution equations of the measures we don't take into account details
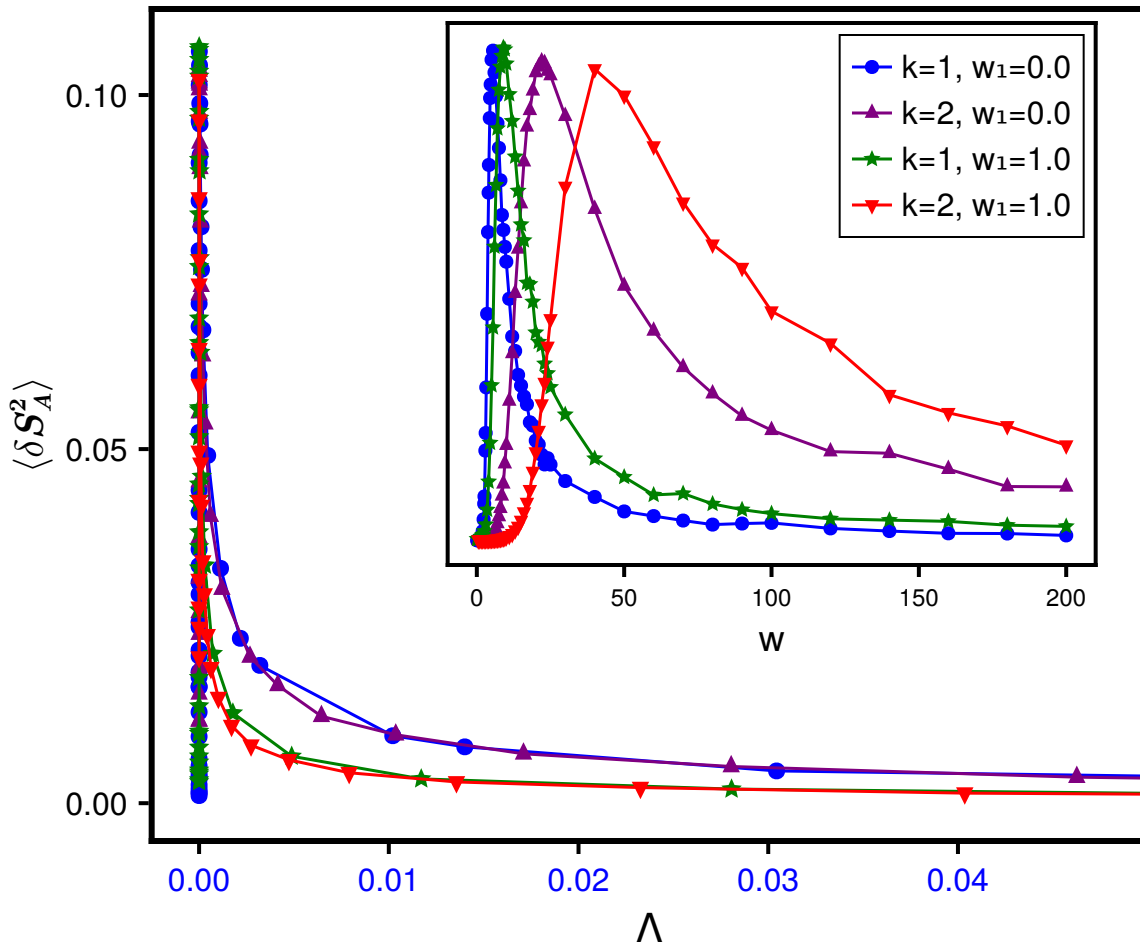
FIG. 7: **Evolution of variance of SPEE.** Following from fig. 6 we show the evolution of the $\langle \delta S_A^2 \rangle$. The details are same as in the fig. 6

of any system at hand, they are applicable to a wide range of many-body systems whose Hamiltonian matrix elements are independent and can be described by a JPDF; the system specific details enter only through Λ. Nonetheless, we have tested our theoretical analysis on a prototypical many-body Hamiltonian - a variant of the QREM - where we study the entanglement dynamics for several system sizes.

We have also analyzed theoretically the SPEE for one-particle systems, and applied it to the entanglement analysis of the 3D Anderson model. Unlike the QREM, we fix the system size in the Anderson model but vary the different parameters present in the system, viz., the number of neighbors, the diagonal disorder strength and the hopping strength. We find that the evolution of the SPEE in systems with different number of neighbors is the same,
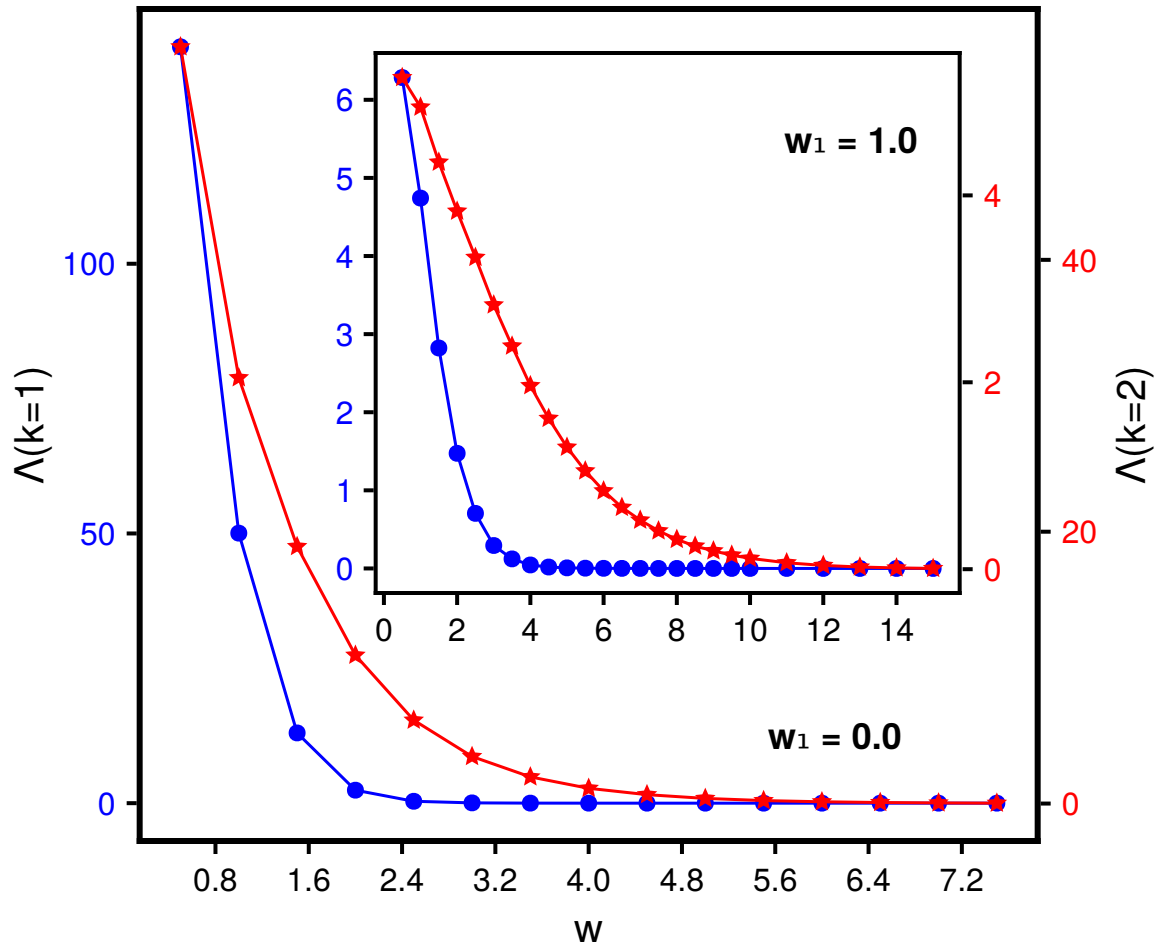
FIG. 8: **Disorder-dependence of** Λ For the various sets of the parameters considered in figs. 6, and 7, the figure displays the complexity parameter Λ with the diagonal disorder parameter w. We note that, while Λ for different k is of the same order, the Λ for different w_1 are apart by an order of magnitude. This, in fact, renders distinguishing evolution for the entanglement for random and non-random hopping in figs. 6 and 7.

however, it's different for systems with random and non-random hopping strength. The latter is attributed to the fact that Λ for random and non-random hopping are quantitatively quite different.

In this work, we have considered many-body systems with uncorrelated matrix elements. However, several systems of physical relevance have highly correlated elements, e.g., the random-filed Heisenberg model [29], the $p-$spin model [36], etc. The complexity-parameter formalism for systems with correlated matrix elements has been discussed in ref. [22]. It's

application to the entanglement dynamics in correlated systems is also very desirable. Furthermore, an extension of the single-parametric formulation of the SPEE to multi-fermionic systems, where the eigenstate is a Slater determinant and the entanglement entropy can be calculated from two-point correlation functions [37–39], is also an interesting path to pursue.

IX. ACKNOWLEDGMENT

[1] K. Życzkowski, K. A. Penson, I. Nechita, and B. Collins, "Generating random density matrices," *Journal of Mathematical Physics*, vol. 52, no. 6, 2011.

[2] C. Nadal, S. N. Majumdar, and M. Vergassola, "Statistical distribution of quantum entanglement for a random bipartite state," *Journal of Statistical Physics*, vol. 142, pp. 403–438, 2011.

[3] S. Kumar and A. Pandey, "Entanglement in random pure states: spectral density and average von neumann entropy," *Journal of Physics A: Mathematical and Theoretical*, vol. 44, no. 44, p. 445301, 2011.

[4] S. N. Majumdar, "Extreme eigenvalues of wishart matrices: application to entangled bipartite system," *arXiv preprint arXiv:1005.4515*, 2010.

[5] B. Collins and I. Nechita, "Random matrix techniques in quantum information theory," *Journal of Mathematical Physics*, vol. 57, 1 2016.

[6] I. Bengtsson and K. Życzkowski, *Geometry of quantum states: an introduction to quantum entanglement.* Cambridge university press, 2017.

[7] D. Shekhar and P. Shukla, "Entanglement dynamics of multi-parametric random states: a single parametric formulation," *Journal of Physics A: Mathematical and Theoretical*, vol. 56, p. 265303, jun 2023.

[8] D. Shekhar and P. Shukla, "Edge of entanglement in non-ergodic states: a complexity parameter formulation," *arXiv preprint arXiv:2310.12796*, 2023.

[9] D. Shekhar and P. Shukla, "Distribution of the entanglement entropy of a non-ergodic quantum state," *arXiv preprint arXiv:2402.01102*, 2024.

[10] P. Shukla, "Eigenfunction statistics of complex systems: A common mathematical formulation," *Physical Review E - Statistical, Nonlinear, and Soft Matter Physics*, vol. 75, 5 2007.

[11] C. R. Laumann, A. Pal, and A. Scardicchio, "Many-body mobility edge in a mean-field quantum spin glass," *Physical Review Letters*, vol. 113, 11 2014.

[12] C. L. Baldwin, C. R. Laumann, A. Pal, and A. Scardicchio, "The many-body localized phase of the quantum random energy model," *Physical Review B*, vol. 93, 1 2016.

[13] G. Biroli, D. Facoetti, M. Schiró, M. Tarzia, and P. Vivo, "Out-of-equilibrium phase diagram of the quantum random energy model," *Physical Review B*, vol. 103, 1 2021.

[14] T. Parolini and G. Mossi, "Multifractal dynamics of the qrem," 7 2020.

[15] P. Shukla, "Level statistics of anderson model of disordered systems: Connection to brownian ensembles," *Journal of Physics Condensed Matter*, vol. 17, pp. 1653–1677, 3 2005.

[16] P. Biswas, P. Cain, R. A. Römer, and M. Schreiber, "Off-diagonal disorder in the anderson model of localization," *Physica Status Solidi (B) Basic Research*, vol. 218, pp. 205–209, 2000.

[17] X. Jia, A. R. Subramaniam, I. A. Gruzberg, and S. Chakravarty, "Entanglement entropy and multifractality at localization transitions," *Physical Review B - Condensed Matter and Materials Physics*, vol. 77, 1 2008.

[18] M. Pouranvari, "Directional localization in disordered 2d tight-binding systems: insights from single-particle entanglement measures," *European Physical Journal B*, vol. 97, 11 2024.

[19] P. Shukla, "Towards a common thread in complexity: an accuracy based approach," *Journal of Physics A: Mathematical and Theorectical*, vol. 41, p. 304023, 2008.

[20] P. Shukla, "Disorder perturbed flat bands: Level density and inverse participation ratio," *Physical Review B*, vol. 98, 8 2018.

[21] P. Shukla, "Level statistics of anderson model of disordered systems: Connection to brownian ensembles," *Journal of Physics Condensed Matter*, vol. 17, pp. 1653–1677, 3 2005.

[22] P. Shukla, "Random matrices with correlated elements: A model for disorder with interactions," *Phys. Rev. E*, vol. 71, p. 026226, Feb 2005.

[23] P. Shukla, "Alternative technique for complex spectra analysis," *Phys. Rev. E*, vol. 62, pp. 2098–2113, Aug 2000.

[24] M. L. Mehta, *Random matrices*. Elsevier, 2004.

[25] F. Haake, *Quantum signatures of chaos*. Springer, 1991.

[26] M. Potters and J.-P. Bouchaud, *A First Course in Random Matrix Theory: For Physicists, Engineers and Data Scientists*. Cambridge University Press, 2020.

[27] D. N. Page, "Average entropy of a subsystem," *Physical review letters*, vol. 71, no. 9, p. 1291, 1993.

[28] E. Bianchi and P. Dona, "Typical entanglement entropy in the presence of a center: Page curve and its variance," *Physical Review D*, vol. 100, no. 10, p. 105010, 2019.

[29] D. J. Luitz, N. Laflorencie, and F. Alet, "Many-body localization edge in the random-field heisenberg chain," *Physical Review B*, vol. 91, no. 8, p. 081103, 2015.

[30] F. Pietracaprina, N. Macé, D. J. Luitz, and F. Alet, "Shift-invert diagonalization of large many-body localizing spin chains," *SciPost Physics*, vol. 5, no. 5, p. 045, 2018.

[31] V. Hernandez, J. E. Roman, and V. Vidal, "SLEPc: A scalable and flexible toolkit for the solution of eigenvalue problems," *ACM Trans. Math. Software*, vol. 31, no. 3, pp. 351–362, 2005.

[32] T. Mondal and P. Shukla, "Spectral statistics of multiparametric gaussian ensembles with chiral symmetry," *Physical Review E*, vol. 102, 9 2020.

[33] R. Horodecki, P. Horodecki, M. Horodecki, and K. Horodecki, "Quantum entanglement," *Reviews of modern physics*, vol. 81, no. 2, pp. 865–942, 2009.

[34] G. De Chiara and A. Sanpera, "Genuine quantum correlations in quantum many-body systems: a review of recent progress," *Reports on Progress in Physics*, vol. 81, no. 7, p. 074002, 2018.

[35] O. Giraud, "Purity distribution for bipartite random pure states," *Journal of Physics A: Mathematical and Theoretical*, vol. 40, no. 49, p. F1053, 2007.

[36] C. L. Baldwin and C. R. Laumann, "Quantum algorithm for energy matching in hard optimization problems," *Physical Review B*, vol. 97, 6 2018.

[37] P. Zanardi, "Quantum entanglement in fermionic lattices," *Physical Review A - Atomic, Molecular, and Optical Physics*, vol. 65, p. 5, 2002.

[38] Y. Zhao, D. Feng, Y. Hu, S. Guo, and J. Sirker, "Entanglement dynamics in the three-dimensional anderson model," *Physical Review B*, vol. 102, 11 2020.

[39] I. Peschel and V. Eisler, "Reduced density matrices and entanglement entropy in free lattice models," *Journal of Physics A: Mathematical and Theoretical*, vol. 42, 2009.

[40] P. Shukla, "Eigenfunction statistics of wishart brownian ensembles," *Journal of Physics A: Mathematical and Theorectical*, vol. 50, p. 435003, 2017.

Appendix A: First and second moments of eigenvalues and eigenfunctions

Consider a $N \times N$ Hermitian matrix $H(Y)$ with Y as a parameter, U as the $N \times N$ eigenvector matrix of $H(Y)$, $(U^\dagger U = 1)$ and E as the $N \times N$ diagonal matrix of its eigenvalues, $E_{mn} = e_n \, \delta_{mn}$. A small change δY in parameter Y changes H and its eigenvalues and eigenfunctions. Using standard perturbation theory for Hermitian operators and by considering matrix $H + \delta H$ in the eigenfunction representation of matrix H, the second order change in the jth component U_{jn} of an eigenfunction U_n , in an arbitrary basis $|j\rangle$, $j = 1, \ldots, N$, due to a small change δY can be described as

$$\delta U_{jn} = \sum_{m \neq n} \frac{\delta H_{mn}}{e_n - e_m} H_{jm} + \sum_{m,m' \neq n}^{N} \frac{\delta H_{mn} \, \delta H_{m'n}}{(e_n - e_m)(e_n - e_{m'})} U_{jm}$$
$$- \sum_{m \neq n}^{N} \frac{\delta H_{mn} \, \delta H_{nn}}{(e_n - e_m)^2} U_{jm} - \frac{1}{2} U_{jn} \sum_{m \neq n}^{N} \frac{\delta H_{mn} \, \delta H_{nm}}{(e_n - e_m)^2} \tag{A1}$$

Similarly a small change δe_n in the eigenvalue e_n can be given as

$$\delta e_n = \delta H_{nn} + \sum_{m \neq n} \frac{|\delta H_{mn}|^2}{e_n - e_m} + o((\delta H_{mn})^3) \tag{A2}$$

where $H_{mn} = e_n \, \delta_{mn}$ at value Y of complexity parameter (due to $H + \delta H$ being considered in the diagonal representation of H).

As discussed in section II of the main text, the Y governed evolution equation for $\rho(H)$ is

$$\frac{\partial \rho}{\partial Y} = \sum_{\mu,\nu} \frac{\partial}{\partial H_{\mu\nu;s}} \left[\frac{g_{\mu\nu}}{2} \frac{\partial}{\partial H_{\mu\nu;s}} + H_{\mu\nu;s} \right] \tag{A3}$$

where with $g_{\mu\nu} = 2$ or 1 for $\mu = \nu$ and $\mu \neq \nu$, respectively,

In general, assuming Markovian process, the parametric diffusion of the joint probability distribution $P_x(x_1, \ldots, x_N; Y)$ of N variables x_n, $n = 1, \ldots, N$ from an arbitrary initial condition, with Y as the parameter, is given by the standard Fokker-Planck approach,

$$\frac{\partial P_x}{\partial Y} \delta Y = \frac{1}{2} \sum_{k,l=1}^{N} \frac{\partial^2}{\partial x_k \partial x_l} \left(\langle \delta x_k \delta x_l \rangle \, P_x \right) - \sum_{k=1}^{N} \frac{\partial}{\partial x_k} \left(\langle \delta x_k \rangle \, P_x \right) \tag{A4}$$

A comparison of eq.(A4) with the above equation thereby gives the relevant information

30

for the moments of $\rho(H)$,

$$\langle \delta H_{\mu\nu;s} \rangle = -\gamma \; H_{\mu\nu;s} \; \delta Y, \tag{A5}$$

$$\langle (\delta H_{\mu\nu;s})^2 \rangle = g_{\mu\nu} \; \delta Y, \qquad \langle (\delta H_{\mu\nu;s} \; \delta H^*_{\mu'\nu';s'} \rangle = 0 \tag{A6}$$

with $g_{\mu\mu} = 2$ and $g_{\mu\nu} = 1$ for $\mu \neq \nu$. All other averages are of a higher order in δY and can be ignored for a small change in Y. Here $\beta = 1, 2$ for H real-symmetric or complex Hermitian, respectively.

An ensemble average of eq.(A1) would lead to moments for the eigenfunction components. This however requires information about the moments of $\langle \delta H^2_{mn} \rangle$ as well as $\langle \delta H_{mn} U_{jm} \rangle$ and $\langle \delta H_{mn} \delta H_{kn} U_{jn} \rangle$. A calculation of these averages is easier if each U_n is represented in a basis $|j\rangle$ in which the perturbation applied to $H(Y)$ is random; this renders the elements of δH matrix statistically independent of the components U_{jn}. (Also note the ensemble averaging is over the ensemble of δH matrices for a fixed H at Y). An appropriate choice for $|j\rangle$ for this purpose is the eigenfunction basis of H_0 at $Y = Y_0 = 0$. Now using eqs.(A5-A6), it is easy to see that the ensemble averaged U_{jn} has a non zero contribution only from the last term of eq.(A1):

$$\langle \delta U_{jn} \rangle = -\beta \; v^2 \sum_{m=1,m\neq n}^{N} \frac{U_{jn} \; \delta Y}{(e_n - e_m)^2} \tag{A7}$$

with angular brackets implying conditional ensemble averages with fixed $e_n, U_n, n = 1, \ldots, N$ and $\beta = 1$ or 2 for H as a real-symmetric or complex Hermitian matrix. But the 2nd moment of the eigenvector components has a contribution only from the first term in eq.(A1) (up to first order in δY) and depends on β:

Case $\beta = 1$

$$\langle \delta U_{jn} \; \delta U_{kl} \rangle = 2 \; v^2 \left(\sum_{m=1,m\neq n}^{N} \frac{U_{jm} \; U_{km} \; \delta_{nl}}{(e_n - e_m)^2} - \frac{U_{jl} \; U_{kn} \; (1 - \delta_{nl})}{(e_n - e_l)^2} \right) \delta Y \tag{A8}$$

Case $\beta = 2$

$$\langle \delta U_{jn} \; \delta U^*_{kl} \rangle = 4 \; v^2 \sum_{m=1,m\neq n}^{N} \frac{U_{jm} \; U^*_{km} \; \delta_{nl} \; \delta Y}{(e_n - e_m)^2}$$

$$\langle \delta U_{jn} \; \delta U_{kl} \rangle = -4 \; v^2 \frac{U_{jl} \; U_{kn} \; (1 - \delta_{nl}) \; \delta Y}{(e_n - e_l)^2} \tag{A9}$$

31

Similarly an ensemble average of eq.(A2) gives, up to first order of δY,

$$\langle \delta e_n \rangle = 2 \beta v^2 \left[N_A - \frac{\gamma}{\beta v^2} e_n + \sum_{m=1, m \neq n}^{N} \frac{1}{e_n - e_m} \right] \delta Y$$

$$\langle \delta e_n \delta e_m \rangle = 8 v^2 e_n \delta_{nm} \delta Y \tag{A10}$$

Further, to first order in δY, the ensemble averaged correlation between $\delta \lambda_k$ and δU_{jn} is zero (for both $\beta = 1$ or 2):

$$\langle \delta e_k \, \delta U_{jn} \rangle = -2 \beta v^2 \sum_{m=1, m \neq n}^{N} \frac{H_{mn}}{(e_n - e_m)} U_{jn} \, \delta Y = 0 \tag{A11}$$

Relevant information from the moments of eigenvalues and eigenfunction components of H can now be derived by using standard Fokker-Planck approach (eq.(A4). As, for finite Y, the moments for the eigenfunction components depend on the eigenvalues too, we first write the diffusion equation for the joint probability density $P_{ef,ev}(\{U_n\}, \{\lambda_n\}; Y)$ at perturbation strength Y where $\{U_n\}$ and $\{\lambda_n\}$ refer to the sets of all eigenvectors $U_1, \ldots, U_N$ and eigenvalues $\lambda_1, \lambda_2, .., \lambda_N$:

$$\frac{\partial P_{ef,ev}}{\partial Y} = (\mathcal{L}_U + \mathcal{L}_U^* + \mathcal{L}_E) P_{ef,ev} \tag{A12}$$

where $\mathcal{L}_U$ and $\mathcal{L}_E$ refer to two parts of the Fokker-Planck operator corresponding to eigenvalues and eigenfunction components, respectively. Here $\mathcal{L}_U$ is given as

$$\mathcal{L}_U \, \delta Y = \frac{\beta}{2} \sum_{j,n=1}^{N} \frac{\partial}{\partial U_{jn}} \left[\frac{\beta}{4} \sum_{k,l=1}^{N} \left(\frac{\partial}{\partial U_{kl}} \langle \delta U_{jn} \delta U_{kl} \rangle + \frac{\partial}{\partial U_{kl}^*} \langle \delta U_{jn} \delta U_{kl}^* \rangle \right) - \langle \delta U_{jn} \rangle \right] \tag{A13}$$

and $\mathcal{L}_E$ is

$$\mathcal{L}_E \, \delta Y = \sum_n \frac{\partial}{\partial e_n} \left[\frac{1}{2} \frac{\partial}{\partial e_n} \langle (\delta e_n)^2 \rangle - \langle \delta e_n \rangle \right] \tag{A14}$$

Note here $P_{ef,ev}$ is subjected to following boundary condition for $\nu = 1$: $P_{ef,ev} \to 0$ for $U_{jn} \to \pm \infty, \lambda_n \to [0, \infty)$ for $j, n = 1 \to N$; this follows because the higher order moments of the ensemble density are assumed to be negligible.

A substitution of the moments (eqs.(A10, A7, A8, A9, A11)) in eq.(A12) followed by latter's integration over all undesired variables will then lead to an evolution equation for the joint probability density of the desired combination of eigenfunctions and eigenvalues.

Appendix B: Joint distribution of all components of an eigenfunction

The relations (A7, A9, A11) describe the moments of the joint probability density function $P_{ef,ev}(U_1, \ldots, U_N, U_1^*, \ldots, U_N^*; e_1, \ldots, e_N)$. Relevant information for the distribution of the components of an arbitrary eigenfunction of H can now be derived as follows.

The JPDF of the components U_{nk}, of an eigenstate, say U_k of H lying between ψ_n and $\psi_n + \mathrm{d}\psi_n$ with $n = 1 \to N$, can be given as

$$P_1(\psi_1, ..., \psi_N; Y) = \int \delta_{\psi,k} \, P_{ef,ev} \, \mathrm{D}\Omega \tag{B1}$$

where $\mathrm{D}\Omega \equiv \prod_{j=1}^N \mathrm{D}\lambda_j \, \prod_{j=1}^N \mathrm{D}^\beta U_j$ is the volume element in the eigenvalue-eigenvector space and

$$\delta_{\psi,k} = \delta(\Psi - U_k) \, \delta^{\beta-1}(\Psi^* - U_k^*) \tag{B2}$$

Partial differentiation of eq.(B1) with respect to Y, subsequent substitution of eq.(A12) and repeated partially integration leads to the diffusion equation for P_{N1}:

$$\frac{\partial P_1}{\partial Y} = F_k + F_k^* \tag{B3}$$

with

$$F_k = \frac{\beta^2}{4} \left[\sum_{m=1}^N \frac{\partial}{\partial \psi_m} \left[\psi_m \, Q_{mm}^{02} \right] + \sum_{m,n=1}^N \frac{\partial^2}{\partial \psi_m \partial \psi_n^*} Q_{mn}^{12} \right], \tag{B4}$$

with

$$Q_{mn;k}^{rs} = \sum_{j;j\neq k} \int \delta_{\psi,k} \frac{(U_{mj} U_{nj}^*)^r}{(e_k - e_j)^s} \, P_{ef,ev} \, \mathrm{D}\Omega, \tag{B5}$$

$$= \sum_{j;j\neq k} \int \frac{(U_{mj} U_{nj}^*)^r}{(e_k - e_j)^s} \, P_{N2} \, \mathrm{d}e_j \, \mathrm{d}e_k \, \mathrm{D}^\beta U_j. \tag{B6}$$

Here $P_2 = P_2(\Psi, \Phi, e, e')$ is the joint probability density of all the components of two eigenvectors Ψ and Φ along with their eigenvalues e and e', respectively:

$$P_2 = \int \delta_{\psi,k} \, \delta_{\phi,j} \, P_{ef,ev} \prod_{l=1}^N \mathrm{d}e_l \, \mathrm{D}^\beta U_l \tag{B7}$$

where $\delta_{\psi,k}$ is defined in eq.(B2). Note

$$P_\Psi(\Psi, e) = \int P_2 \, \mathrm{d}e' \, \mathrm{D}^\beta \Phi \tag{B8}$$

Eq.(B3) is derived from eq.(A12) without any approximation. The same equation for P_Ψ (with notation P_Ψ replaced by P_{N1} and ψ_m by z_{mk}) was derived in [10] (see eq.(18) of [10]).

As clear from eqs.(B4, B6), the right side of eq.(B3) contains functions which are not explicitly written in terms of P_{N1}. In [10], eq.(B6) was approximated as $Q_{mn;k}^{rs} \approx \frac{(N-1)^{1-r}}{\Delta_k^s} \left(\delta_{mn} - \psi_m^* \psi_n\right)^r P_\Psi$ with Δ_e as the local mean level spacing at energy e (see eq.(22) of [10]). The approximation was however based on an assumed weak statistical correlation between the eigenvalues and the eigenfunctions. Here we consider its improvement to include more generic regimes, based on the following ideas: (i) the eigenvalues at a distance more than few mean level spacing are uncorrelated, (ii) the average correlation between components of an eigenfunction is almost same as another eigenfunction if their eigenvalues are approximately equal. Using these ideas, it can be shown that (see Appendix D of [40] for details)

$$Q_{mn;k}^{rs} \approx \mathcal{K}_s \left(\overline{\langle \psi_n \psi_m^* \rangle}\right)^r P_\Psi(\Psi, e) \tag{B9}$$

where

$$\mathcal{K}_s(e) = \left(\frac{2}{E_c}\right)^s N, \tag{B10}$$

where E_c is an important system-specific spectral-range defined as follows: the eigenvalues at distances more than E_c around e, are uncorrelated. (Note, in context of disordered systems, E_c is also referred as the Thouless energy and is of the order of local mean level spacing Δ_e).

Substitution of the approximations (B9) in eqs.(B4) helps to express F_k in terms of P_Ψ:

$$F_k = \frac{\beta^2 \, \mathcal{K}_2}{4} \sum_{n=1}^N \frac{\partial}{\partial \psi_n} \left[\sum_m \overline{\langle \psi_n \psi_m^* \rangle} \, \frac{\partial P_\Psi}{\partial \psi_m^*} + \psi_n \, P_\Psi \right] \tag{B11}$$

With help of eq.(B11), eq.(B3) reduces now to a differential equation for P_Ψ only.

The evolution equation for the JPDF of the components $\psi_\mu \equiv \langle \mu | \Psi \rangle$ of an arbitrary eigenfuntion Ψ of a Hamiltonian H taken from the ensemble $\rho(H)$ can be given as

$$\frac{\partial P_\Psi}{\partial Y} = \frac{\beta^2 \, \chi_0}{4 \, \Delta_{local}^2} \left(F_\Psi + F_\Psi^*\right) \tag{B12}$$

$F_\Psi \equiv \left[\sum_{m,n} \frac{\partial^2}{\partial \psi_\mu^* \partial \psi_\nu} h_2 + \sum_n \frac{\partial}{\partial \psi_\nu} h_1 \right]$, where, $h_1 \equiv (N-1)\psi_\nu P_\Psi$ and $h_2 \equiv (\delta_{\mu\nu} - \psi_\mu^* \psi_\nu) P_\Psi$ and $\Lambda = \frac{\chi \beta^2}{2\Delta^2}$. We note $F_\Psi = F_\Psi^*$ for $\beta = 1$.

In the bipartite basis, we have $\psi_\mu \equiv C_{mk}, \psi_\nu \equiv C_{nl}$, such that, $m, n = 1 \cdots N_A$, $k, l = 1 \cdots N_B$, and $N = N_A N_B$. The evolution equation for the JPDF P_Ψ for the components

of an arbitrary eigenfunction Ψ of H taken from the ensemble $\rho(H)$ can still be given by eq.(B12). For clarity purposes, F_Ψ can then be rewritten as

$$F_\Psi \equiv \sum_{m,n} \frac{\partial^2}{\partial C_{mk}^* \partial C_{nl}} h_2 + \sum_n \frac{\partial}{\partial C_{nl}} h_1 \tag{B13}$$

with $h_1 \equiv (N-1)C_{nl}P_\Psi$ and $h_2 \equiv (\delta_{mn}\delta_{kl} - C_{mk}C_{nl})P_\Psi$.

A comparison of the above equation with eq.(A4) gives

$$\langle \delta C_{nk} \delta C_{ml} \rangle = \frac{\beta^2 \chi_0}{4\Delta_{local}^2} (\delta_{mn}\delta_{kl} - C_{nk}C_{ml}) \, \delta Y \tag{B14}$$

$$\langle \delta C_{nk} \rangle = -\frac{\beta^2 \chi_0}{4\Delta_{local}^2} (N-1)C_{nk} \, \delta Y. \tag{B15}$$

Except for the correlation term, the above equation is analogous to eq.() in [7]. The JPDF of the Schmidt eiegnvalues can therefore be derived as in [7]; to keep the work self-content here we review the relevant steps.

Eq.(B3) was derived in [10] from another route and eq.(B4) approximately reduce to eq.(23) of [10] if one substitutes $\langle \psi_n \psi_m^* \rangle \approx \frac{1}{N} \, \delta_{mn}$ in eq.(B11). The latter approximation is valid for almost extended eigenfunctions which was the basis of derivation in [10].

Appendix C: Evolution of the JPDF of Schmidt Eigenvalues

Assuming the Markovian dynamics, the evolution can be described by a standard Fokker-Planck equation

$$\frac{\partial P_\lambda}{\partial \Lambda} \delta\Lambda = \frac{1}{2} \sum_{m,n} \frac{\partial^2}{\partial \lambda_m \partial \lambda_n} (\langle \delta\lambda_n \delta\lambda_m \rangle P_\lambda) - \sum_n \frac{\partial}{\partial \lambda_n} (\langle \delta\lambda_n \rangle P_\lambda). \tag{C1}$$

Here the required moments of the eigenvalues can be determined as follows. The second order spectral perturbation theory of the Hermitian matrices gives

$$\delta\lambda_n = \delta W_{nn} + \sum_{m(\neq n)} \frac{(\delta W_{mn})^2}{\lambda_n - \lambda_m} + \mathcal{O}(\delta W_{mn}^3), \tag{C2}$$

with W as the reduced density matrix for subsystem A. The above on ensemble averaging leads to

$$\langle \delta\lambda_n \rangle = \beta \langle \delta W_{nn} \rangle + \sum_{m(\neq n)} \frac{\langle |\delta W_{mn}|^2 \rangle}{\lambda_n - \lambda_m} \tag{C3}$$

$$\langle \delta\lambda_n \delta\lambda_m \rangle = \langle \delta W_{nn} \delta W_{mm} \rangle \tag{C4}$$

To proceed further, we need to determine the moments $\langle \delta W_{nn} \rangle$, $\langle |\delta W_{mn}|^2 \rangle$ and $\langle \delta W_{nn} \delta W_{mm} \rangle$.

The reduced density matrix W is defined as $W = CC^\dagger$; a perturbation of C is therefore expected to manifest in W too. As expected, the diffusive dynamics of the matrix elements C_{kl} manifests itself in the W-matrix space. The moments for the matrix elements $W_{mn} = \sum_{k=1}^{N_A} C_{km}^* C_{kn}$ can be calculated from those of C. The above equations along with relation between the elements of C and W gives the moments of the matrix elements of W as (with $W = W^\dagger$), with $\Lambda = \frac{\chi_0}{\Delta_{local}^2}$,

$$\langle \delta W_{mm} \rangle = -(N-1) W_{mm} \delta\Lambda. \tag{C5}$$

$$\langle \delta W_{mn} \, \delta W_{mn}^* \rangle = [\beta (W_{mm} + W_{nn}) - 4 W_{mm} W_{nn}] \, \delta\Lambda \tag{C6}$$

$$\langle \delta W_{mm} \, \delta W_{nn} \rangle = -4 \, W_{mm} \, W_{nn} \, \delta\Lambda \tag{C7}$$

Substitution of the above relations in eq.(C3) and eq.(C4) leads to

$$\langle \delta\lambda_n \rangle = \beta \left[-(N-1)\lambda_n + \sum_{m(\neq n)} \frac{\lambda_n + \lambda_m}{\lambda_n - \lambda_m} \right] \delta\Lambda, \tag{C8}$$

$$\langle \delta\lambda_n \delta\lambda_m \rangle = 4 \left(\delta_{mn} \lambda_n - \lambda_n \lambda_m \right) \delta\Lambda \tag{C9}$$

A substitution of the above moments in eq.(C1) now leads to eq.(21).

Appendix D: Evolution of entanglement measures (S_2 and R_1)

Consider a function $f(\Lambda) \equiv f(\lambda_1, \ldots, \lambda_N) = \sum_k f_k(\lambda_k)$. From the eq. (21) of the main text, we can write,

$$\frac{\partial \langle f(\Lambda) \rangle}{\partial \Lambda} = \int f(\Lambda) \frac{\partial P_\lambda}{\partial \Lambda} D_\lambda = I_1 + I_2 + I_3, \tag{D1}$$

36

where,

$$I_1 = \sum_n \int \frac{\partial^2}{\partial \lambda_n^2}[(\lambda_n - \lambda_n^2)P_\lambda]\, f(\Lambda)\, D_\lambda \tag{D2}$$

$$= \sum_n \int (\lambda_n - \lambda_n^2)\, P_\lambda \left(\frac{\partial^2 f}{\partial \lambda_n^2}\right) D_\lambda \tag{D3}$$

$$I_2 = -\sum_{m \neq n} \int \frac{\partial^2}{\partial \lambda_n \partial \lambda_m}(\lambda_n \lambda_m P_\lambda)S_2 D_\lambda \tag{D4}$$

$$= \sum_{m \neq n} \int \lambda_n \lambda_m \left(\frac{\partial^2 f}{\partial \lambda_m \partial \lambda_n}\right) P_\lambda D_\lambda \tag{D5}$$

$$I_3 = -\beta \sum_n \int \frac{\partial}{\partial \lambda_n}\left[\left(\sum_{m(\neq n)} \frac{\lambda_n}{\lambda_n - \lambda_m} - \nu - \frac{N}{2}\lambda_n\right) P_\lambda\right] f(\lambda)\, D_\lambda \tag{D6}$$

$$= \beta \int \left[\left(\sum_{m(\neq n)} \frac{\lambda_n}{\lambda_n - \lambda_m} - \nu - \frac{N}{2}\lambda_n\right)\right] \left(\frac{\partial f}{\partial \lambda_n}\right) P_\lambda D_\lambda. \tag{D7}$$

The evolution of various measures e.g. purity S_2 and R_1 can now be obtained by substitution of their expression in terms of Schmidt eigenvalues.

Λ**-dependence of** $\langle S_2 \rangle$: Using $S_2 = \sum_{n=1}^{N} \lambda_n^2$ in eqs. (D3), (D5), and (D7), we have $I_1 = 2 - 2\langle S_2 \rangle$, $I_2 = 0$ and $I_3 = 2\beta\left[(N_A - \nu - 1) - \frac{N}{2\beta}\langle S_2 \rangle\right]$. These on substitution in eq. (D1) give

$$\frac{\partial \langle S_2 \rangle}{\partial \Lambda} = a - b\langle S_2 \rangle; \qquad a = N_A + N_B + 1,\ b = N_A N_B + 2. \tag{D8}$$

The above equation can be solved, using the initial conditions $\langle S_2 \rangle(\Lambda = 0) = 1$, to arrive at

$$\langle S_2 \rangle = \frac{a}{b}(1 - e^{-b\Lambda}) + e^{-b\Lambda} \tag{D9}$$

Λ**-dependence of** $\langle S_3 \rangle$: Using $S_3 = \sum_{n=1}^{N} \lambda_n^3$ in eqs. (D3), (D5), and (D7), we have $I_1 = 6(\langle S_2 \rangle - \langle S_3 \rangle)$, $I_2 = 0$ and $I_3 = 3\beta\left[(N_A - \nu - \frac{3}{2}) - \frac{N}{2\beta}\langle S_3 \rangle + \frac{1}{2}\right]$. These on substitution in eq. (D1) give

$$\frac{\partial \langle S_3 \rangle}{\partial \Lambda} = \frac{3}{2}(a+1)\langle S_2 \rangle - \frac{3}{2}b\langle S_3 \rangle + \frac{3}{2}. \tag{D10}$$

In fact, we conjecture,

$$\frac{\partial \langle S_n \rangle}{\partial \Lambda} = \frac{n}{2}\left[(a + (n-2))\langle S_{n-1} \rangle - b\langle S_n \rangle + (n-2)\langle S_{n-2} \rangle\right]. \tag{D11}$$

Using eq. (D9) in the above equation, and then solving using the initial condition $\langle S_3 \rangle(\Lambda = 0) = 1$, we get,

$$\langle S_3 \rangle = \frac{1}{b^2}\left(a^2 + b + (2a^2 - 3ab + b^2 - b)e^{-\frac{3}{2}b\Lambda} + 3a(b-a)e^{-b\Lambda}\right). \tag{D12}$$

Also as $\Lambda \to \infty$, $\langle S_3 \rangle \to \frac{1}{N_A^2}$.

Λ-dependence of S_2-variance: Using $S_2^2 = \sum_{m,n=1}^{N} \lambda_n^2 \lambda_m^2$ in eqs. (D3), (D5), and (D7), we have $I_1 = 8\langle S_3 \rangle + 4\langle S_2 \rangle - 8\langle S_4 \rangle - 4\langle S_2^2 \rangle$, $I_2 = -8\langle S_2^2 \rangle + 8\langle S_4 \rangle$ and $I_3 = 4\beta(N_A - \nu - 1)\langle S_2 \rangle - \frac{N}{2\beta}\langle S_2^2 \rangle$. These on substitution in eq. (D8) give

$$\frac{\partial \langle S_2^2 \rangle}{\partial \Lambda} = 8\langle S_3 \rangle - 2b\langle S_2^2 \rangle + 2a\langle S_2 \rangle, \tag{D13}$$

where, a and b are as defined in eq. (D8).

Using the definition $\langle \delta S_2^2 \rangle = \langle S_2^2 \rangle - \langle S_2 \rangle^2 \Rightarrow$, the evolution of variance can be given as

$$\frac{\partial \langle \delta S_2^2 \rangle}{\partial \Lambda} = \frac{\partial \langle S_2^2 \rangle}{\partial \Lambda} - 2\langle S_2 \rangle \frac{\partial \langle S_2 \rangle}{\partial \Lambda} \tag{D14}$$

$$\Rightarrow \frac{\partial \langle \delta S_2^2 \rangle}{\partial \Lambda} = -2\,b\,\langle \delta S_2^2 \rangle + 8\langle S_3 \rangle, \tag{D15}$$

where, in obtaining the last equality we have used eqs. (D8) and eq. (D13). We note from eq. (D15) that the variance depends on higher order S_n, i.e., S_3.

Now we can use the eq. (D12) in eq. (D15), and solve the latter using the initial condition $\langle \delta S_2^2 \rangle(\Lambda = 0) = 0$, to get

$$\langle \delta S_2^2(\Lambda) \rangle = \frac{4e^{-2b\Lambda}}{b^3} \left(e^{\frac{b\Lambda}{2}} - 1 \right) \left(-5a^2 e^{\frac{b\Lambda}{2}} + a^2 e^{\frac{3b\Lambda}{2}} + a^2 e^{b\Lambda} + 3a^2 + 6\,a\,b\,e^{\frac{b\Lambda}{2}} \right.$$
$$\left. - 6\,a\,b + 4b^2 + b\,e^{\frac{b\Lambda}{2}} + b\,e^{\frac{3b\Lambda}{2}} + b\,e^{b\Lambda} - 3b \right).$$

Λ-dependence of $\langle R_1 \rangle$: Using $R_1 = -\sum_{n=1}^{N} \lambda_n$ in eqs. (D3), (D5), and (D7), we have $I_1 = -(N_A - 1)$, $I_2 = 0$ and $I_3 \approx -N_A(N_A - 1) + \frac{N}{2} + N_A\nu + \frac{N_B}{2}\langle R_0 \rangle - \frac{N}{2}\langle R_1 \rangle$ where, I_3 has been obtained by the approximation $\sum_{m \neq n} \frac{\lambda_n \log \lambda_n}{\lambda_n - \lambda_m} = \frac{N_A(N_A - 1)}{2} - (\frac{N_A - 1}{2})R_0$, and $R_0 \equiv -\sum_n \log \lambda_n$ (see Appendix J of [7]). These on substitution in eq. (D1) now give

$$\frac{\partial \langle R_1 \rangle}{\partial \Lambda} = -(N_A^2 - 1) + \frac{N}{2} + N_A\nu + \frac{N_B}{2}\langle R_0 \rangle - \frac{N}{2}\langle R_1 \rangle. \tag{D16}$$

The above equation gives the correct limiting behaviour for R_1: as $\Lambda \to \infty$, $\langle R_0 \rangle \to N_A \log N_A + \frac{N_A^2}{2N_B}$ [7], and $\langle R_1 \rangle \to \log N_A - \frac{N_A}{2N_B} - \frac{1}{N_B}$, which is the Page limit [27]. Further, as noticed in an earlier study, $\langle R_0 \rangle$ has a very weak dependence on Λ and it tends to be a constant in the $N \to \infty$ limit, assuming $\langle R_0 \rangle$ to be a constant, equal to its steady state value, we can solve the above eq. (D16) to obtain,

$$\langle R_1(\Lambda) \rangle = R_{1,\infty}(1 - e^{-\frac{N\Lambda}{2}}), \tag{D17}$$

where, $R_{1,\infty} = R_{\text{page}} \approx \log N_A - \frac{N_A}{2N_B}$

Λ-**dependence of** R_1-**variance**: Using $R_1^2 = \sum_{m,n=1}^N \lambda_n \lambda_m \, \log \lambda_m \lambda_n$ in eqs. (D3), (D5), and (D7), we have $I_1 + I_2 = 2Q - 2\langle R_1^2 \rangle - 2(N_A - 1)\langle R_1 \rangle$, where, $Q \equiv \langle \sum_n \lambda_n (\log \lambda_n)^2 \rangle$ and $I_3 = -N_A(N_A - 1)\langle R_1 \rangle + N_B \langle R_0 R_1 \rangle - N \langle R_1^2 \rangle$. These on substitution in eq. (D1) give

$$\frac{\partial \langle R_1^2 \rangle}{\partial \Lambda} = 2Q - (N_A - 1)(N_A + 2)\langle R_1 \rangle + N_B \langle R_0 R_1 \rangle - (N + 2)\langle R_1^2 \rangle. \tag{D18}$$

Finally, since $\langle \delta R_1^2 \rangle \equiv \langle R_1^2 \rangle - \langle R_1 \rangle^2$, using eqs. (D16) and (D18), we get,

$$\begin{aligned} \frac{\partial \langle \delta R_1^2 \rangle}{\partial \Lambda} &= \frac{\partial \langle R_1^2 \rangle}{\partial \Lambda} - 2\langle R_1 \rangle \frac{\partial \langle R_1 \rangle}{\partial \Lambda} \\ &= 2(Q - \langle R_1^2 \rangle) + N_B \, \mathrm{cov}(R_0, R_1) - N \langle \delta R_1^2 \rangle, \end{aligned} \tag{D19}$$

where, the covarinace $\mathrm{cov}(R_0, R_1) \equiv \langle R_0 R_1 \rangle - \langle R_0 \rangle \langle R_1 \rangle$.

Appendix E: Entanglement in Anderson Model

An eigenstate of the single-particle Anderson Hamiltonian can be written in the site basis as,

$$|\psi\rangle = \sum_{r \in A \cup B} \psi(r) |1\rangle_r \otimes_{r' \neq r} |0\rangle_{r'}, \tag{E1}$$

where, A and B are the two bi-partitions, created, for example, slicing the 3D lattice horizontally. The above state can then be written as a superposition of states where the particle occupies either the subsystem A or B:

$$|\psi\rangle = |1\rangle_A |0\rangle_B + |0\rangle_A + |1\rangle_B, \tag{E2}$$

where, $|1\rangle_A = \sum_{r \in A} \psi(r) |1\rangle \otimes_{r' \neq r} |0\rangle_{r'}$ and $|0\rangle_A = \otimes_{r \in A} |0\rangle_r$; similarly, for B. We define,

$$P_A \equiv \langle 1|1\rangle_A = \sum_{r \in A} |\psi(r)|^2, \tag{E3}$$

1. Dynamics of P_A

We can work out the complete dynamics of P_A from the JPDF of eigenfunction components,

$$\frac{\partial P_N}{\partial \Lambda} = \sum_{m,n} \frac{\partial^2}{\partial z_n \partial z_m} h_2 + \sum_n \frac{\partial}{\partial z_n} h_1, \tag{E4}$$

where, $h_1 \equiv (N-1) z_n P_N$, and $h_2 \equiv (\delta_{mn} - z_n z_m) P_N$. We have,

$$\frac{\partial \langle P_A \rangle}{\partial \Lambda} = \int P_A \frac{\partial P_N}{\partial \Lambda} D_z. \tag{E5}$$

Again, by repeated partial integration, we get,

$$\frac{\partial \langle P_A \rangle}{\partial \Lambda} = 2(N_A - N\langle P_A \rangle). \tag{E6}$$

At first, we can see that, since for the balanced bi-partition $N = 2N_A$, we have, as $\Lambda \to \infty, \langle P_A \rangle \to 0.5$. Further, for solving eq. (E6), we need to choose the initial condition carefully. $\Lambda \to 0$ correspond to the localized state. The localization center can, however, belong to either region A or B, depending on which, P_A is either 0 or 1. The presence or absence of the localization center in region A is a completely random event.

For analyzing the statistics of P_A, in this work, for a fixed set of parameters, we filter eigenstates from all the samples (set of states near $E = 0$ for a disorder realization and for many such disorder realizations) whose localization center lie in A; such that we have, $\langle P_A \rangle (\Lambda = 0) = 1$. With this, we can solve eq. (E6) to get,

$$\langle P_A(\Lambda) \rangle = \frac{1}{2} \left[1 + e^{-4N_A \Lambda} \right]. \tag{E7}$$

2. Dynamics of SPEE

We have,

$$S_A(\rho_A) = -P_A \log P_A - P_B \log P_B, \tag{E8}$$

where, $P_B \equiv 1 - P_A$. For deriving the evolution equation for $\langle S_A \rangle$, we note the following,

$$\frac{\partial S_A}{\partial z_n} = \begin{cases} -2z_n \log P_A - 2z_n, & n \in A \\ -2z_n \log P_B - 2z_n, & n \in B \end{cases} \tag{E9}$$

and,

$$\frac{\partial^2 S_A}{\partial z_m z_n} = \begin{cases} -2(1 + \log P_A)\delta_{mn} - \frac{4z_n z_m}{P_A}, & m,n \in A \\ -2(1 + \log P_B)\delta_{mn} - \frac{4z_n z_m}{P_B}, & m,n \in B \\ -4z_n z_m \log P_A, & n \in A; m \in B \\ -4z_n z_m \log P_B, & n \in B; m \in A. \end{cases} \tag{E10}$$

Since,

$$\frac{\partial \langle S_A \rangle}{\partial \Lambda} = \int S_A \frac{\partial P_N}{\partial \Lambda} D_z, \tag{E11}$$

using eq. B12 and the relations eqs. (E9) and (E10) in the above equation and performing repeated partial integrations we get,

$$\frac{\partial \langle S_A \rangle}{\partial \Lambda} = -4 - 2N \langle S_A \rangle - \int (N + 4P_A P_B) \log P_A P_B. \tag{E12}$$

Further, since $0 \leq 4P_A P_B \leq 1, \Rightarrow N \gg 4P_A P_B$, we can simplify the above equation to get,

$$\frac{\partial \langle S_A \rangle}{\partial \Lambda} = -4 - 2N \langle S_A \rangle - N \langle \log P_A P_B \rangle. \tag{E13}$$

3. Dynamics of $P_A P_B$

From eq. (35) of the main text, we get, for $k = 1$,

$$\frac{\partial \langle P_A P_B \rangle}{\partial \Lambda} = N - 4(N + 2)\langle P_A P_B \rangle \tag{E14}$$

$$\Rightarrow \langle P_A P_B \rangle = \frac{N}{4(N + 2)} \left[1 - e^{-4(N+2)\Lambda} \right]. \tag{E15}$$

The above equation correctly gives that in the ergodic limit $\Lambda \to \infty$, $\langle P_A P_B \rangle \approx \frac{1}{4}$. Similarly, for $k = 2$,

$$\frac{\partial \langle (P_A P_B)^2 \rangle}{\partial \Lambda} = 2(N + 4)\langle P_A P_B \rangle - 8(N + 6)\langle (P_A P_B)^2 \rangle. \tag{E16}$$

Further, using the eqs. (E14) and (E16), we get the evolution equation for the variance,

$$\frac{\partial \langle \delta(P_A P_B)^2 \rangle}{\partial \Lambda} = 8\langle P_A P_B \rangle - 48\langle (P_A P_B)^2 \rangle + 16\langle P_A P_B \rangle^2 - 8N \langle \delta(P_A P_B)^2 \rangle, \tag{E17}$$

which can be solved and simplified to get,

$$\langle \delta(P_A P_B)^2 \rangle = \frac{1}{16N^3} \left[8N + 8N(N + 4)e^{-4(N+2)\Lambda} - N(N^2 + 16N)e^{-8(N+2)\Lambda} + N(N^2 + 8N)e^{-8(N+6)\Lambda} \right]. \tag{E18}$$